AUTHOR QUERY FORM

ELSEVIER	Journal: EABE Article Number: 2298	Please e-mail or fax your responses and any corrections to: E-mail: corrections.eseo@elsevier.macipd.com Fax: +44 1392 285878

Dear Author,

Any queries or remarks that have arisen during the processing of your manuscript are listed below and highlighted by flags in the proof. Please check your proof carefully and mark all corrections at the appropriate place in the proof (e.g., by using on-screen annotation in the PDF file) or compile them in a separate list.

For correction or revision of any artwork, please consult http://www.elsevier.com/artworkinstructions.

Articles in Special Issues: Please ensure that the words 'this issue' are added (in the list and text) to any references to other articles in this Special Issue

Uncited references: References that occur in the reference list but not in the text – please position each reference in the text or delete it from the list.	
Missing references: References listed below were noted in the text but are missing from the reference list – please make the list complete or remove the references from the text.	
Location in article	**Query/remark** **Please insert your reply or correction at the corresponding line in the proof**
Q1	Please check correspondence address.
Q2	Please provide the significance of 'underline' in Tables 2 and 7.
Q3	Please provide journal name for Ref. [3].
Q4	Please update Refs. [43,47].
Q5	Because of unbreakable equations, we typeset this article in single column. Please check.
Q6	Please confirm the insertion of brackets in Eqs. (4.8, 4.11, 4.17).
Q7	Please confirm the deletion of bracket in Eq. (4.18).

Electronic file usage

Sometimes we are unable to process the electronic file of your article and/or artwork. If this is the case, we have proceeded by:

☐ Scanning (parts of) your article ☐ Rekeying (parts of) your article ☐ Scanning the artwork

Thank you for your assistance.

Engineering Analysis with Boundary Elements ■ (■■■■) ■■■–■■■

Contents lists available at ScienceDirect

Engineering Analysis with Boundary Elements

journal homepage: www.elsevier.com/locate/enganabound

Combined Trefftz methods of particular and fundamental solutions for corner and crack singularity of linear elastostatics

Ming-Gong Lee [a], Lih-Jier Young [a], Zi-Cai Li [a,*], Po-Chun Chu [a,b,c]

[a] Department of Applied Mathematics, Chung Hua University, Hsin-Chu, Taiwan
[b] Department of Applied Mathematics, National Sun Yat-sen University, Kaohsiung 80424, Taiwan
[c] Department of Computer Science and Engineering, National Sun Yat-sen University, Kaohsiung 80424, Taiwan

ARTICLE INFO

Article history:
Received 22 December 2009
Accepted 15 February 2010

Keywords:
Elastostatics
Trefftz method
Method of fundamental solutions
Crack singularity
Collocation Trefftz method
Combined method

ABSTRACT

The singular solutions at corners and the fundamental solution are *essential* in both theory and computation. Our recent efforts are made to seek new models of corner and crack singularity of linear elastostatics and their numerical solutions. In Li et al. (2009) [43], a systematic analysis for singularity properties and particular solutions of linear elastostatics is explored. This paper is a continued study of Li et al. (2009) [43], *general* singular solutions for corners with free traction boundary conditions are derived. Both particular solutions and fundamental solutions are explored for plane strain and plane stress problems, and the singular solutions are derived directly from linear elastostatics. Two new models (symmetric and anti-symmetric) of interior crack singularities are proposed, and their highly accurate solutions can be found by the collocation Trefftz method. Moreover, for the corner and crack singularity problems, the combined methods by using many fundamental solutions, but by adding *a few* singular solutions are proposed. Such a kind of combined methods is significant for linear elastostatics with corners (i.e., the L-shaped domain), because the singular solutions can be obtained only by seeking the power ν_k of r^{ν_k} numerically (as shown in Li et al., 2009 [43]). Hence, only a few singular solutions used may greatly simplify the numerical algorithms, thus to enrich the numerical solutions of linear elastostatics with corners, and to extend the method of fundamental solutions (MFS) for singularity problems.

1. Introduction

The singular properties and particular solutions (PS) at corners and the fundamental solutions (FS) for linear elastostatics are *essential* in both theory and computation. Our recent efforts are made to seek new models of corner and crack singularity of linear elastostatics and their numerical solutions. In [43], the basic approaches for singularity properties and singular solutions are explored, and two interior crack (i.e., crack tip) models by mimicking Motz's problem are designed. This paper is a continued study of [43]. The first goal is to seek the *general* singular solutions of linear elastostatics near the corners under free traction boundary conditions, which yields a new anti-symmetric model of singularity (cf. [43]) in Section 4.2. The singular properties in Williams [67,48] are obtained by using a similarity to biharmonic equations, and some following discussions are found in Lin and Tong [48], Jirousek and Venkstesh [27], Jirousek and Wroblewski [28] and Qin [60]. In this paper, we will derive the particular solutions directly from the Cauchy–Navier equation of linear elastostatics. Note that our results are also coincident with those in [67,48].

By following [43], the second goal is to design more effective models of crack singularity under free traction boundary conditions. Two new models (symmetric and anti-symmetric) are proposed by mimicking the cracked-beam as in [51], and their highly accurate numerical solutions are obtained by the collocation Trefftz method (CTM). The third goal is to explore systematically the fundamental solutions (FS) of linear elastostatics. The particular solutions and fundamental solutions can be used for plane strain and plane stress problems, to lead to the method of particular solutions (MPS) and the method of fundamental solutions (MFS), respectively. For the crack models, we may develop the combined Trefftz method (TM) with a few singular particular solutions (PS) and many fundamental solutions (FS), to well suit for linear elastostatics with corners. Note that the explicit particular solutions can be found only for the crack tip (i.e., $\Theta=\pi$). For other corners, such as the L-shaped domain, the complex powers ν_k of the functions r^{ν_k} in the corner particular

* Corresponding author at: Department of Applied Mathematics, National Sun Yat-sen University, Kaohsiung 80424, Taiwan.
E-mail addresses: mglee@chu.edu.tw (M.-G. Lee), zcli@math.nsysu.edu.tw (Z.-C. Li).

0955-7997/$ - see front matter © 2010 Published by Elsevier Ltd.
doi:10.1016/j.enganabound.2010.02.005

solutions can only be obtained numerically. On the other hand, the method of fundamental method (MFS) provides poor accuracy of numerical solutions for singularity problems, because the smooth particular solutions cannot fit well with the singular solutions. A better strategy is that only a few corner singular PS are chosen in the combined Trefftz method. For the singularity corners, the technique by adding a few singular solutions was used for finite element method [38], the radial basis function [26,44], the hybrid Trefftz method [22], and the fundamental solutions in their algorithms [3,30], where only one singular solution is added in.

The singular analysis and computation of linear elastostatics at corners are *essential* in both theory and computation. Once the singularity of corner solutions is known, the reduced convergence rates of FEM, FDM and FVM are found, and some improved techniques, such as the combined Trefftz method in this paper (see [38]) can be explored to recover the optimal convergence rates. More importantly, based on the explicit particular solutions of corners given in this paper, we may develop a number of efficient (even new) numerical methods for linear elastostatics, such as the combined method in [36,38,39,41], and the Trefftz methods [2,56,70], which include the boundary approximate method [38], the collocation Trefftz method [25,44], the hybrid Trefftz method (see [12,21,24,22,29,54,60,59]), the boundary collocation techniques [32], etc. Note that this paper also provides a *systematic* analysis of the Trefftz methods using PS and FS for singularity problems of linear elastostatics.

This paper is organized as follows. In Section 2, a basic description for elastostatics problems in 2D is introduced, and the particular solutions are provided. In Section 3, the complex representation of solutions and stress are explored, and the singular solutions near corners are derived for free traction boundary conditions. In Section 4, two models (symmetric and anti-symmetric) of crack singularity are designed, and in Section 5 the collocation Trefftz method (CTM) as in [38,44] is chosen by using particular solutions only, to lead to the method of particular solutions (MPS). In Section 6, the fundamental solutions are explored, and in Section 7, for the crack models of singularity, the combined Trefftz methods with many FS and a few singular PS are also proposed, and numerical experiments are carried out for these two models. A few concluding remarks are made in the last section.

2. Linear elastostatics problems in 2D

2.1. Basic equations

Consider the linear elastostatics problem in 2D. Denote the displacement vector,

$$\vec{w} = \mathbf{w} = \{w_1(\mathbf{x}), w_2(\mathbf{x})\}^T = \{u(x,y), v(x,y)\}^T, \tag{2.1}$$

where $\vec{x} = \mathbf{x} = (x_1, x_2) = (x,y)$. The linear strain tensor is given by

$$\varepsilon_{ij}(\mathbf{x}) = \frac{1}{2}\left[\frac{\partial w_i(\mathbf{x})}{\partial x_j} + \frac{\partial w_j(\mathbf{x})}{\partial x_i}\right], \quad 1 \le i,\ j \le 2. \tag{2.2}$$

Let σ_{ij} $(1 \le i,j \le 2)$ denote the stress tensor at $\mathbf{x}$. For an isotropic homogeneous Hookean solid, there exist the stress–strain relations

$$\sigma_{ij} = \lambda(\nabla \cdot \vec{w})\delta_{ij} + 2\mu\varepsilon_{ij}, \quad 1 \le i,\ j \le 2, \tag{2.3}$$

where " $\nabla \cdot$ " is the divergence operator, δ_{ij} are the Kronecker delta, and λ and μ are the Lamé constants.

When there exists a body force $\vec{f}$, we obtain the non-homogeneous equation,

$$\mu\Delta\vec{w} + (\lambda+\mu)\nabla(\nabla \cdot \vec{w}) + \vec{f} = 0 \quad \text{in } S. \tag{2.4}$$

When $\vec{f} \equiv \vec{0}$, we have the Cauchy–Navier equation of linear elastostatics for isotropic body:

$$\Delta\vec{w} + \frac{1}{1-2v}\nabla(\nabla \cdot \vec{w}) = 0 \quad \text{in } S, \tag{2.5}$$

where the Poisson ratio

$$v = \frac{\lambda}{2(\lambda+\mu)}, \quad 0 < v < \frac{1}{2}. \tag{2.6}$$

Young's modulus E and the bulk modulus K are introduced by

$$E = \frac{\mu(3\lambda+2\mu)}{\lambda+\mu}, \quad K = \frac{E}{3(1-2v)}. \tag{2.7}$$

The inverse relations of (2.6) and (2.7) are given by

$$\lambda = \frac{Ev}{(1+v)(1-2v)}, \quad \mu = \frac{E}{2(1+v)}. \tag{2.8}$$

The strain–stress relations are given by

$$\varepsilon_{ij} = \frac{1+v}{E}\sigma_{ij} - \frac{v}{E}\delta_{ij}\sum_{k=1}^{2}\sigma_{kk}. \tag{2.9}$$

There also exist the symmetric relations:

$$\sigma_{ij} = \sigma_{ji}, \quad \varepsilon_{ij} = \varepsilon_{ji}. \tag{2.10}$$

Denote the constant

$$\kappa = \frac{1}{4(1-v)}. \tag{2.11}$$

Please cite this article as: Lee M-G, et al. Combined Trefftz methods of particular and fundamental solutions for corner and crack singularity of linear elastostatics. Eng Anal Bound Elem (2010), doi:10.1016/j.enganabound.2010.02.005

For the plane strain problem the constant

$$D=\frac{\lambda+\mu}{\lambda+3\mu}=\frac{1}{3-4v}=\frac{\kappa}{1-\kappa}, \tag{2.12}$$

where κ is given in (2.11), and for the plane stress problem,

$$D=\frac{1}{3-4v}=\frac{1+\hat{v}}{3-\hat{v}}, \quad v=\frac{\hat{v}}{1+\hat{v}}. \tag{2.13}$$

We cite a result in Chen and Zhou [7, p. 513–5], as a theorem.

Theorem 2.1. *The general solutions of the linear elastostatic equation ([illegible]) in 2D are given by*

$$\vec{w}(\vec{x})=\vec{h}(\vec{x})-\kappa\nabla[\vec{x}\cdot\vec{h}(\vec{x})+q(\vec{x})], \tag{2.14}$$

where $\vec{h}(\vec{x})$ is the harmonic vector and $q(\vec{x})$ is a harmonic function. When $q(\vec{x})\equiv 0$, the functions in (2.14) from $\vec{h}(\vec{x})$ only are called the principal particular solutions.

2.2. Traction boundary conditions

The Cauchy–Navier equation (2.5) is written explicitly as

$$\mu\Delta u+(\lambda+\mu)\left\{\frac{\partial^2 u}{\partial x^2}+\frac{\partial^2 v}{\partial x\partial y}\right\}=0 \quad \text{in } S, \tag{2.15}$$

$$\mu\Delta v+(\lambda+\mu)\left\{\frac{\partial^2 u}{\partial x\partial y}+\frac{\partial^2 v}{\partial y^2}\right\}=0 \quad \text{in } S, \tag{2.16}$$

or by

$$\Delta u+\frac{1}{1-2v}\left\{\frac{\partial^2 u}{\partial x^2}+\frac{\partial^2 v}{\partial x\partial y}\right\}=0 \quad \text{in } S, \tag{2.17}$$

$$\Delta v+\frac{1}{1-2v}\left\{\frac{\partial^2 u}{\partial x\partial y}+\frac{\partial^2 v}{\partial y^2}\right\}=0 \quad \text{in } S, \tag{2.18}$$

where v is given in (2.6). The traction on ∂S is denoted by

$$\vec{\tau}(\vec{w})(\mathbf{x})=(\tau_1(u,v),\tau_2(u,v))^T, \tag{2.19}$$

where the components are given by

$$\tau_1(u,v)=\sigma_x n_1+\sigma_{xy}n_2=\lambda\left(\frac{\partial u}{\partial x}+\frac{\partial v}{\partial y}\right)n_1+2\mu\frac{\partial u}{\partial v}+\mu n_2\left(\frac{\partial v}{\partial x}-\frac{\partial u}{\partial y}\right), \tag{2.20}$$

$$\tau_2(u,v)=\sigma_{xy}n_1+\sigma_y n_2=\lambda\left(\frac{\partial u}{\partial x}+\frac{\partial v}{\partial y}\right)n_2+2\mu\frac{\partial v}{\partial v}-\mu n_1\left(\frac{\partial v}{\partial x}-\frac{\partial u}{\partial y}\right), \tag{2.21}$$

where $n_1=\cos(v,x)$, $n_2=\cos(v,y)$, and the stress

$$\sigma_x=\sigma_{11}, \quad \sigma_y=\sigma_{22}, \quad \sigma_{xy}=\sigma_{12}. \tag{2.22}$$

2.3. Particular solutions

From Muskhelishvili's complex variable formula [53] (also see Qin [60]), the solution of linear elastostatics can be expressed in the complex function

$$u+iv=\phi(z)-Dz\overline{\phi'(z)}-\overline{\psi}(z), \tag{2.23}$$

where the complex functions $z=x+iy$, $\overline{z}=x-iy$ and $i=\sqrt{-1}$. In (2.23), $\phi(z)$ and $\psi(z)$ are two analytic functions.

In Jirousek and Wroblewski [28], Jirousek and Venkstesh [27] and Qin [60], for the plane stress equations (2.17) and (2.18), the particular solutions are expressed as the complex functions. The particular solutions $u(x,y)$ and $v(x,y)$ of the plane stress equations are given by the real and imaginary parts of A_k, B_k, C_k and D_k below, respectively,

$$A_k=iz^{\mu_k}+iD\mu_k z\overline{z}^{\mu_k-1}, \tag{2.24}$$

$$B_k=z^{\mu_k}-D\mu_k z\overline{z}^{\mu_k-1}, \tag{2.25}$$

$$C_k=i\overline{z}^{\mu_k}, \tag{2.26}$$

$$D_k=-\overline{z}^{\mu_k}, \quad k=1,2,\ldots, \tag{2.27}$$

Please cite this article as: Lee M-G, et al. Combined Trefftz methods of particular and fundamental solutions for corner and crack singularity of linear elastostatics. Eng Anal Bound Elem (2010), doi:10.1016/j.enganabound.2010.02.005

where the complex $\mu_k=\alpha_k+i\beta_k$, $\alpha_k,\beta_k\in\Re$, and D is given in (2.12) and (2.13) for strain and stress problems, respectively. We have the following linear combination for the Trefftz method (TM):

$$u_L=\sum_{k=1}^{L}\{a_k\Re(A_k)+b_k\Re(B_k)+c_k\Re(C_k)+d_k\Re(D_k)\}+d_0, \tag{2.28}$$

$$v_L=\sum_{k=1}^{L}\{a_k\Im(A_k)+b_k\Im(B_k)+c_k\Im(C_k)+d_k\Im(D_k)\}+c_0, \tag{2.29}$$

where a_k, b_k, c_k and d_k are the constants, and the notations $\Re$ and $\Im$ are the real and the imaginary parts, respectively. In (2.28) and (2.29) $u=\Re(A_1)=-(1+D)y$ and $v=\Im(A_1)=(1+D)x$ denote a rigid motion.

The singularity solutions can be obtained from (2.24) to (2.27) as the following:

$$u_L=\sum_{k=1}^{L}r^{\mu_k}\{a_k[-\sin\mu_k\theta+D\mu_k\sin(\mu_k-2)\theta]+b_k[\cos\mu_k\theta-D\mu_k\cos(\mu_k-2)\theta]+c_k\sin\mu_k\theta-d_k\cos\mu_k\theta\}+d_0, \tag{2.30}$$

$$v_L=\sum_{k=1}^{L}r^{\mu_k}\{a_k[\cos\mu_k\theta+D\mu_k\cos(\mu_k-2)\theta]+b_k[\sin\mu_k\theta+D\mu_k\sin(\mu_k-2)\theta]+c_k\cos\mu_k\theta+d_k\sin\mu_k\theta\}+c_0. \tag{2.31}$$

3. Singularity near corners

3.1. Complex presentations of solutions and stress

We will follow the analytic approaches as in [43] for seeking the general solutions at corners with the free traction boundary conditions. Using complex representations of solutions and stress is convenient to find the particular solutions in applications. We have the following lemma.

Lemma 3.1. *For* (2.5) *of linear elastostatics in 2D, the principal particular solutions of* (2.14) *and* (2.23) *with* $\overline{\psi}(z)\equiv 0$ *are equivalent to each other.*[1]

Proof. Below we show the equivalence of two principal terms,

$$u+iv=\phi(z)-Dz\overline{\phi'(z)}, \tag{3.1}$$

where $\phi(z)=u^*+iv^*$ is an analytic function, and

$$\vec{w}(\vec{x})=\vec{h}(\vec{x})-\kappa\nabla[\vec{x}\cdot\vec{h}(\vec{x})], \tag{3.2}$$

where $\vec{h}(\vec{x})=(u^*,v^*)^T$ is the harmonic vector, and the constant $\kappa=1/4(1-\nu)$. From (3.2) we have

$$\begin{pmatrix}u\\ v\end{pmatrix}=(1-\kappa)\begin{pmatrix}u^*\\ v^*\end{pmatrix}-\kappa\begin{pmatrix}x\dfrac{\partial u^*}{\partial x}+y\dfrac{\partial v^*}{\partial x}\\ x\dfrac{\partial u^*}{\partial y}+y\dfrac{\partial v^*}{\partial y}\end{pmatrix}. \tag{3.3}$$

Take the plane strain problem for example. Since $D=(\lambda+\mu)/(\lambda+3\mu)=\kappa/(1-\kappa)$, it is sufficient to show

$$z\overline{\phi'(z)}=(xu_x^*+yv_x^*)+i(xu_y^*+yv_y^*). \tag{3.4}$$

From $z=x+iy$ and $\overline{z}=x-iy$, we have

$$\frac{\partial}{\partial x}=\frac{\partial}{\partial z}+\frac{\partial}{\partial\overline{z}},\quad \frac{\partial}{\partial y}=i\left(\frac{\partial}{\partial z}-\frac{\partial}{\partial\overline{z}}\right), \tag{3.5}$$

and then

$$\frac{\partial}{\partial z}=\frac{1}{2}\left(\frac{\partial}{\partial x}-i\frac{\partial}{\partial y}\right),\quad \frac{\partial}{\partial\overline{z}}=\frac{1}{2}\left(\frac{\partial}{\partial x}+i\frac{\partial}{\partial y}\right). \tag{3.6}$$

Moreover for solutions u^* and v^*, the Cauchy equalities hold,

$$u_x^*=v_y^*,\quad v_x^*=-u_y^*. \tag{3.7}$$

Then we have from (3.6)

$$\phi'(z)=\frac{\partial}{\partial z}\phi(z)=\frac{1}{2}\left(\frac{\partial}{\partial x}-i\frac{\partial}{\partial y}\right)(u^*+iv^*)=\frac{1}{2}\{(u_x^*+v_y^*)+i(v_x^*-u_y^*)\}. \tag{3.8}$$

From (3.7), Eq. (3.8) leads to

$$\phi'(z)=u_x^*-iu_y^*. \tag{3.9}$$

[1] The proof for the equivalence of the other (i.e., minor) terms of (2.14) and (2.23) is given in [46].

Please cite this article as: Lee M-G, et al. Combined Trefftz methods of particular and fundamental solutions for corner and crack singularity of linear elastostatics. Eng Anal Bound Elem (2010), doi:10.1016/j.enganabound.2010.02.005

Hence we obtain

$$\begin{aligned} z\overline{\phi'(z)} &= (x+iy)(u_x^*+iu_y^*) = (xu_x^*-yu_y^*)+i(yu_x^*+xu_y^*) \\ &= (xu_x^*+yv_x^*)+i(xu_y^*+yv_y^*), \end{aligned} \tag{3.10}$$

where we have used (3.7) again. This is the desired result (3.4), and completes the proof of Lemma 3.1. □

Lemma 3.2. *For plane stress problems, under the particular solutions* (2.23), *there exist the stress formulas* (*also see* [69,53]),

$$\sigma_x = \Re(2\phi'(z)-\bar{z}\phi''(z)-\psi'(z)), \tag{3.11}$$

$$\sigma_y = \Re(2\phi'(z)+\bar{z}\phi''(z)+\psi'(z)), \tag{3.12}$$

$$\sigma_{xy} = \Im(\bar{z}\phi''(z)+\psi'(z)). \tag{3.13}$$

Proof. We have from (2.23)

$$u = \frac{1}{2\mu}\Re\left\{\frac{\lambda+3\mu}{\lambda+\mu}\phi(z)-\bar{z}\phi'(z)-\psi(z)\right\}, \tag{3.14}$$

$$v = \frac{1}{2\mu}\Im\left\{\frac{\lambda+3\mu}{\lambda+\mu}\phi(z)+\bar{z}\phi'(z)+\psi(z)\right\}. \tag{3.15}$$

There exist the stress formulas,

$$\sigma_x = (\lambda+2\mu)u_x+\lambda v_y, \tag{3.16}$$

$$\sigma_y = \lambda u_x+(\lambda+2\mu)v_y, \tag{3.17}$$

$$\sigma_{xy} = \mu(u_y+v_x). \tag{3.18}$$

From (3.5), (3.14) and (3.15), we have

$$\begin{aligned} \sigma_x &= (\lambda+2\mu)\left(\frac{\partial}{\partial z}+\frac{\partial}{\partial \bar{z}}\right)u+\lambda i\left(\frac{\partial}{\partial z}-\frac{\partial}{\partial \bar{z}}\right)v \\ &= \frac{\lambda+2\mu}{2\mu}\Re\left\{\frac{\lambda+3\mu}{\lambda+\mu}\phi'(z)-\bar{z}\phi''(z)-\phi'(z)-\psi'(z)\right\}+\frac{\lambda}{2\mu}\Re\left\{\frac{\lambda+3\mu}{\lambda+\mu}\phi'(z)+\bar{z}\phi''(z)-\phi'(z)+\psi'(z)\right\} \\ &= \Re(2\phi'(z)-\bar{z}\phi''(z)-\psi'(z)). \end{aligned} \tag{3.19}$$

Similarly, we have

$$\begin{aligned} \sigma_y &= \lambda\left(\frac{\partial}{\partial z}+\frac{\partial}{\partial \bar{z}}\right)u+(\lambda+2\mu)i\left(\frac{\partial}{\partial z}-\frac{\partial}{\partial \bar{z}}\right)v \\ &= \frac{\lambda}{2\mu}\Re\left\{\left(\frac{\lambda+3\mu}{\lambda+\mu}-1\right)\phi'(z)-\bar{z}\phi''(z)-\psi'(z)\right\}+\frac{\lambda+2\mu}{2\mu}i\Im\left\{\left(\frac{\lambda+3\mu}{\lambda+\mu}-1\right)\phi'(z)+\bar{z}\phi''(z)+\psi'(z)\right\} \\ &= \frac{\lambda}{\lambda+\mu}\Re\{\phi'(z)\}+\frac{\lambda}{2\mu}\Re\{-\bar{z}\phi''(z)-\psi'(z)\}+\frac{\lambda+2\mu}{\lambda+\mu}\Re\{\phi'(z)\}+\frac{\lambda+2\mu}{2\mu}\Re\{\bar{z}\phi''(z)+\psi'(z)\} \\ &= \Re(2\phi'(z)+\bar{z}\phi''(z)+\psi'(z)), \end{aligned} \tag{3.20}$$

and

$$\begin{aligned} \sigma_{xy} &= \mu\left\{i\left(\frac{\partial}{\partial z}-\frac{\partial}{\partial \bar{z}}\right)u+\left(\frac{\partial}{\partial z}+\frac{\partial}{\partial \bar{z}}\right)v\right\} \\ &= i\mu\frac{1}{2\mu}\Re\left\{\left(\frac{\lambda+3\mu}{\lambda+\mu}+1\right)\phi'(z)-\bar{z}\phi''(z)-\psi'(z)\right\}+\mu\frac{1}{2\mu}\Im\left\{\left(\frac{\lambda+3\mu}{\lambda+\mu}+1\right)\phi'(z)+\bar{z}\phi''(z)+\psi'(z)\right\} \\ &= \Im(\bar{z}\phi''(z)+\psi'(z)). \end{aligned} \tag{3.21}$$

This completes the proof of Lemma 3.2. □

Based on Lemma 3.2, we have the stress formulas

$$\begin{pmatrix} \sigma_x \\ \sigma_y \\ \sigma_{xy} \end{pmatrix} = \vec{T}_i, \quad i = 1,2,3,4, \tag{3.22}$$

where[2]

$$\vec{T}_1=\begin{pmatrix}\Re R_{1k}-\Re S_{1k}\\ \Re R_{1k}+\Re S_{1k}\\ \Im S_{1k}\end{pmatrix},\quad R_{1k}=2Di\mu_k z^{\mu_k-1},\quad S_{1k}=iD\mu_k(\mu_k-1)z^{\mu_k-2}\overline{z}, \tag{3.23}$$

$$\vec{T}_2=\begin{pmatrix}\Re R_{2k}-\Re S_{2k}\\ \Re R_{2k}+\Re S_{2k}\\ \Im S_{2k}\end{pmatrix},\quad R_{2k}=2D\mu_k z^{\mu_k-1},\quad S_{2k}=D\mu_k(\mu_k-1)z^{\mu_k-2}\overline{z}, \tag{3.24}$$

$$\vec{T}_3=\begin{pmatrix}-\Re S_{3k}\\ \Re S_{3k}\\ \Im S_{3k}\end{pmatrix},\quad S_{3k}=i\mu_k z^{\mu_k-1}, \tag{3.25}$$

and

$$\vec{T}_4=\begin{pmatrix}-\Re S_{4k}\\ \Re S_{4k}\\ \Im S_{4k}\end{pmatrix},\quad S_{4k}=\mu_k z^{\mu_k-1}. \tag{3.26}$$

Hence we have from (3.22) to (3.26)

$$\sigma_x=\sum_{k=1}^{\infty}\mu_k r^{\mu_k-1}\{a_kD[-2\sin(\mu_k-1)\theta+(\mu_k-1)\sin(\mu_k-3)\theta]+b_kD[2\cos(\mu_k-1)\theta-(\mu_k-1)\cos(\mu_k-3)\theta]+c_k\sin(\mu_k-1)\theta-d_k\cos(\mu_k-1)\theta\}, \tag{3.27}$$

$$\sigma_y=\sum_{k=1}^{\infty}\mu_k r^{\mu_k-1}\{-a_kD[2\sin(\mu_k-1)\theta+(\mu_k-1)\sin(\mu_k-3)\theta]+b_kD[2\cos(\mu_k-1)\theta+(\mu_k-1)\cos(\mu_k-3)\theta]-c_k\sin(\mu_k-1)\theta+d_k\cos(\mu_k-1)\theta\}, \tag{3.28}$$

$$\sigma_{xy}=\sum_{k=1}^{\infty}\mu_k r^{\mu_k-1}\{a_kD(\mu_k-1)\cos(\mu_k-3)\theta+b_kD(\mu_k-1)\sin(\mu_k-3)\theta+c_k\cos(\mu_k-1)\theta+d_k\sin(\mu_k-1)\theta\}. \tag{3.29}$$

The corner singularity of elasticity plane was first discussed in Williams [67] and Lin and Tong [48], and then in Jirousek and Wroblewski [28], Jirousek and Venkstesh [27] and Qin [60]. Note that Eqs. (3.22)–(3.26) directly from the Cauchy–Navier equation are coincident with [27,60, p. 82].

3.2. Particular solutions near corners

In this section, we will also derive the particular solutions for the corners with free traction boundary conditions. Choose the sectorial domain $S=\{(r,\theta)|(0\le R,-\Theta\le\theta\le\Theta)\}$, where $\Theta\in(0,\pi]$. First consider the free stress conditions at two edges of the corner O with

$$\tau_x=\tau_y=0\quad\text{on }\theta=\pm\Theta, \tag{3.30}$$

where the stress formulas are given by

$$\tau_x=\sigma_x\cos(n,x)+\sigma_{xy}\cos(n,y), \tag{3.31}$$

$$\tau_y=\sigma_{xy}\cos(n,x)+\sigma_y\cos(n,y). \tag{3.32}$$

For the exterior normal $\vec{n}$ of the edge boundary, we have

$$\cos(n,x)=\cos\left(\frac{\pi}{2}+\theta\right)=-\sin\theta, \tag{3.33}$$

$$\cos(n,y)=\cos\theta. \tag{3.34}$$

Hence we have from (3.30)

$$\tau_x=-\sigma_x\sin\theta+\sigma_{xy}\cos\theta=0, \tag{3.35}$$

$$\tau_y=-\sigma_{xy}\sin\theta+\sigma_y\cos\theta=0. \tag{3.36}$$

Based on (3.27)–(3.29) we have from (3.31) and (3.32),

$$\tau_x=\sum_{k=1}^{\infty}\mu_k r^{\mu_k-1}\{a_kD[2\sin(\mu_k-1)\theta\sin\theta+(\mu_k-1)\cos(\mu_k-2)\theta]+b_kD[-2\cos(\mu_k-1)\theta\sin\theta+(\mu_k-1)\sin(\mu_k-2)\theta]+c_k\cos\mu_k\theta+d_k\sin\mu_k\theta\}, \tag{3.37}$$

$$\tau_y=\sum_{k=1}^{\infty}\mu_k r^{\mu_k-1}\{-a_kD[2\sin(\mu_k-1)\theta\cos\theta+(\mu_k-1)\sin(\mu_k-2)\theta]+b_kD[2\cos(\mu_k-1)\theta\cos\theta+(\mu_k-1)\cos(\mu_k-2)\theta]-c_k\sin\mu_k\theta+d_k\cos\mu_k\theta\}. \tag{3.38}$$

From (3.37) and (3.38) we have the matrix equation

$$\mathbf{By}=\mathbf{0}, \tag{3.39}$$

[2] In this paper, we use the complex numbers μ_k and μ^*, different from the constant μ.

Please cite this article as: Lee M-G, et al. Combined Trefftz methods of particular and fundamental solutions for corner and crack singularity of linear elastostatics. Eng Anal Bound Elem (2010), doi:10.1016/j.enganabound.2010.02.005

where $\mathbf{y}=(a,b,c,d)^T$, the matrix is given by

$$\mathbf{B}=\begin{pmatrix} b_{11} & b_{12} & \cos\mu^*\Theta & \sin\mu^*\Theta \\ b_{21} & b_{22} & -\sin\mu^*\Theta & \cos\mu^*\Theta \\ b_{11} & -b_{12} & \cos\mu^*\Theta & -\sin\mu^*\Theta \\ -b_{21} & b_{22} & \sin\mu^*\Theta & \cos\mu^*\Theta \end{pmatrix},$$

and the entries are given by

$$b_{11}=2D\sin(\mu^*-1)\Theta\sin\Theta+D(\mu^*-1)\cos(\mu^*-2)\Theta,$$

$$b_{12}=-2D\cos(\mu^*-1)\Theta\sin\Theta+D(\mu^*-1)\sin(\mu^*-2)\Theta,$$

$$b_{21}=-2D\sin(\mu^*-1)\Theta\cos\Theta-D(\mu^*-1)\sin(\mu^*-2)\Theta,$$

$$b_{22}=2D\cos(\mu^*-1)\Theta\cos\Theta+D(\mu^*-1)\cos(\mu^*-2)\Theta. \tag{3.40}$$

We have a lemma, whose proof is similar to [43].

Lemma 3.3. *For nonzero solutions of the equations*

$$\begin{pmatrix} b_{11} & b_{12} & b_{13} & b_{14} \\ b_{21} & b_{22} & b_{23} & b_{24} \\ b_{11} & -b_{12} & b_{13} & -b_{14} \\ -b_{21} & b_{22} & -b_{23} & b_{24} \end{pmatrix}\begin{pmatrix} a \\ b \\ c \\ d \end{pmatrix}=\vec{0}, \tag{3.41}$$

there exist the equalities

$$\begin{vmatrix} b_{11} & b_{13} \\ b_{21} & b_{23} \end{vmatrix}=0,\quad \begin{vmatrix} b_{12} & b_{14} \\ b_{22} & b_{24} \end{vmatrix}=0. \tag{3.42}$$

Based on Lemma 3.3, the non-zero solutions of (3.39) satisfy two equations:

$$\begin{vmatrix} b_{11} & \cos\mu^*\Theta \\ b_{21} & -\sin\mu^*\Theta \end{vmatrix}=D\begin{vmatrix} 2\sin(\mu^*-1)\Theta\sin\Theta+(\mu^*-1)\cos(\mu^*-2)\Theta & \cos\mu^*\Theta \\ -[2\sin(\mu^*-1)\Theta\cos\Theta+(\mu^*-1)\sin(\mu^*-2)\Theta] & -\sin\mu^*\Theta \end{vmatrix}=0, \tag{3.43}$$

$$\begin{vmatrix} b_{12} & \sin\mu^*\Theta \\ b_{22} & \cos\mu^*\Theta \end{vmatrix}=D\begin{vmatrix} [-2\cos(\mu^*-1)\Theta\sin\Theta+(\mu^*-1)\sin(\mu^*-2)\Theta] & \sin\mu^*\Theta \\ 2\cos(\mu^*-1)\Theta\cos\Theta+(\mu^*-1)\cos(\mu^*-2)\Theta & \cos\mu^*\Theta \end{vmatrix}=0. \tag{3.44}$$

We will simplify the above two equations. First, to simplify (3.43) we have

$$(2\sin(\mu^*-1)\Theta\sin\Theta+(\mu^*-1)\cos(\mu^*-2)\Theta)(-\sin\mu^*\Theta)=-[2\sin(\mu^*-1)\Theta\cos\Theta+(\mu^*-1)\sin(\mu^*-2)\Theta]\cos\mu^*\Theta, \tag{3.45}$$

to give

$$-2\sin(\mu^*-1)\Theta[\sin\Theta\sin\mu^*\Theta-\cos\mu^*\Theta\cos\Theta]=(\mu^*-1)(\cos(\mu^*-2)\Theta\sin\mu^*\Theta-\cos\mu^*\Theta\sin(\mu^*-2)\Theta), \tag{3.46}$$

and then

$$2\cos(\mu^*+1)\Theta\sin(\mu^*-1)\Theta=(\mu^*-1)\sin2\Theta. \tag{3.47}$$

By using the trigonometric formulas

$$\begin{aligned}\cos(\mu^*+1)\Theta&=\cos\mu^*\Theta\cos\Theta-\sin\mu^*\Theta\sin\Theta,\\ \sin(\mu^*-1)\Theta&=\sin\mu^*\Theta\cos\Theta-\cos\mu^*\Theta\sin\Theta,\end{aligned} \tag{3.48}$$

the left side of (3.47) leads to

$$2\sin\mu^*\Theta\cos\mu^*\Theta(\cos^2\Theta+\sin^2\Theta)-2\cos\Theta\sin\Theta(\cos^2\mu^*\Theta+\sin^2\mu^*\Theta)=\sin2\mu^*\Theta-\sin2\Theta. \tag{3.49}$$

Then we have from (3.47)

$$\sin2\mu^*\Theta=\mu^*\sin2\Theta. \tag{3.50}$$

Next, to simplify (3.44) we have

$$[-2\cos(\mu^*-1)\Theta\sin\Theta+(\mu^*-1)\sin(\mu^*-2)\Theta]\cos\mu^*\Theta=(2\cos(\mu^*-1)\Theta\cos\Theta+(\mu^*-1)\cos(\mu^*-2)\Theta)\sin\mu^*\Theta, \tag{3.51}$$

to give

$$-2\cos(\mu^*-1)\Theta(\cos\Theta\sin\mu^*\Theta+\sin\Theta\cos\mu^*\Theta)=(\mu^*-1)(-\sin(\mu^*-2)\Theta\cos\mu^*\Theta+\cos(\mu^*-2)\Theta\sin\mu^*\Theta), \tag{3.52}$$

and then

$$-2\cos(\mu^*-1)\Theta\sin(\mu^*+1)\Theta=(\mu^*-1)\sin 2\Theta. \tag{3.53}$$

By using the trigonometric formulas

$$\begin{aligned}&\cos(\mu^*-1)\Theta=\cos\mu^*\Theta\cos\Theta+\sin\mu^*\Theta\sin\Theta,\\&\sin(\mu^*+1)\Theta=\sin\mu^*\Theta\cos\Theta+\cos\mu^*\Theta\sin\Theta,\end{aligned} \tag{3.54}$$

the left side of (3.53) leads to

$$-2\sin\mu^*\Theta\cos\mu^*\Theta(\cos^2\Theta+\sin^2\Theta)-2\cos\Theta\sin\Theta(\cos^2\mu^*\Theta+\sin^2\mu^*\Theta)=-\sin 2\mu^*\Theta-\sin 2\Theta. \tag{3.55}$$

Then we have from (3.53)

$$-\sin 2\mu^*\Theta=\mu^*\sin 2\Theta. \tag{3.56}$$

Combining (3.50) and (3.56) yields the following theorem.

Theorem 3.1. *Let* (3.39) *be given for the free stress conditions* (3.30). *There exist the equalities*

$$\sin 2\mu^*\Theta=\pm\mu^*\sin 2\Theta, \tag{3.57}$$

where the signs "$-$" and "+" are for the symmetric and the antisymmetric cases, respectively.

Proof. We only show the sign respondence. The equality (3.57) with sign "$-$" results from (3.56), which denotes the nonzero coefficients b_k and d_k of symmetric solutions u, v in (2.30) and (2.31) satisfying $u_y=v=0$ at $\theta=0$. Also the equality (3.57) with the sign "+" responds to the anti-symmetric solutions u,v satisfying $u=v_y=0$ at $\theta=0$. This completes the proof of Theorem 3.1.

When the complex roots $\mu^*=\mu_k$ (or the real roots in special cases) are obtained from (3.57), the coefficients satisfy the following relations:

$$c_k=p_k^*Da_k,\quad d_k=q_k^*Db_k, \tag{3.58}$$

where p_k and q_k are complex given by

$$p_k^*=-\mu_k\cos 2\Theta+\sqrt{1-(\mu_k\sin 2\Theta)^2}, \tag{3.59}$$

$$q_k^*=-\left\{\mu_k\cos 2\Theta+\sqrt{1-(\mu_k\sin 2\Theta)^2}\right\}. \tag{3.60}$$

Then the particular solutions of (2.30) and (2.31) are then simplified as

$$u_L=\sum_{k=1}^{L}\Re r^{\mu_k}a_k[(-1+Dp_k^*)\sin\mu_k\theta+D\mu_k\sin(\mu_k-2)\theta]+b_k[(1-Dq_k^*)\cos\mu_k\theta-D\mu_k\cos(\mu_k-2)\theta]+b_0, \tag{3.61}$$

$$v_L=\sum_{k=1}^{L}\Re r^{\mu_k}a_k[(1+Dp_k^*)\cos\mu_k\theta+D\mu_k\cos(\mu_k-2)\theta]+b_k[(1+Dq_k^*)\sin\mu_k\theta+D\mu_k\sin(\mu_k-2)\theta]+a_0, \tag{3.62}$$

which also coincide with Lin and Tong [48] and Qin [60].

Below, we prove (3.59) and (3.60) under the assumptions:

$$\cos\mu^*\Theta\neq 0,\quad \sin\mu^*\Theta\neq 0. \tag{3.63}$$

The relation between coefficients a and c can be found in (3.43) under (3.50)

$$c=-\frac{1}{\cos\mu^*\Theta}[2D\sin(\mu^*-1)\Theta\sin\Theta+D(\mu^*-1)\cos(\mu^*-2)\Theta]a=p^*(\mu^*)Da, \tag{3.64}$$

to give

$$\begin{aligned}p^*(\mu^*)&=-\frac{1}{\cos\mu^*\Theta}[2\sin(\mu^*-1)\Theta\sin\Theta+(\mu^*-1)\cos(\mu^*-2)\Theta]\\&=-\frac{1}{\cos\mu^*\Theta}\{2(\sin\mu^*\Theta\cos\Theta-\cos\mu^*\Theta\sin\Theta)\sin\Theta\\&\quad+(\mu^*-1)(\cos\mu^*\Theta\cos 2\Theta+\sin\mu^*\Theta\sin 2\Theta)\}\\&=2\sin^2\Theta-(\mu^*-1)\cos 2\Theta-\frac{\sin\mu^*\Theta}{\cos\mu^*\Theta}[2\cos\Theta\sin\Theta+(\mu^*-1)\sin 2\Theta]\\&=1-\mu^*\cos 2\Theta-\frac{\sin\mu^*\Theta}{\cos\mu^*\Theta}\mu^*\sin 2\Theta.\end{aligned} \tag{3.65}$$

From (3.50) we have

$$p^*(\mu^*)=1-\mu^*\cos 2\Theta-2\sin^2\mu^*\Theta=-\mu^*\cos 2\Theta+\cos 2\mu^*\Theta=-\mu^*\cos 2\Theta+\sqrt{1-(\mu^*\sin 2\Theta)^2}. \tag{3.66}$$

Please cite this article as: Lee M-G, et al. Combined Trefftz methods of particular and fundamental solutions for corner and crack singularity of linear elastostatics. Eng Anal Bound Elem (2010), doi:10.1016/j.enganabound.2010.02.005

This is the first formula (3.59). Next for coefficients b and d, we have from (3.44) under (3.56),

$$d=-\frac{1}{\sin\mu^*\Theta}[-2\cos(\mu^*-1)\Theta\sin\Theta+(\mu^*-1)\sin(\mu^*-2)\Theta]Db=q^*(\mu^*)Db, \tag{3.67}$$

to give

$$\begin{aligned}q^*(\mu^*)&=-\frac{1}{\sin\mu^*\Theta}[-2\cos(\mu^*-1)\Theta\sin\Theta+(\mu^*-1)\sin(\mu^*-2)\Theta]\\&=-\frac{1}{\sin\mu^*\Theta}\{-2(\cos\mu^*\Theta\cos\Theta+\sin\mu^*\Theta\sin\Theta)\sin\Theta+(\mu^*-1)(\sin\mu^*\Theta\cos2\Theta-\cos\mu^*\Theta\sin2\Theta)\}\\&=2\sin^2\Theta-(\mu^*-1)\cos2\Theta+\frac{\cos\mu^*\Theta}{\sin\mu^*\Theta}(2\cos\Theta\sin\Theta+(\mu^*-1)\sin2\Theta)\\&=1-\mu^*\cos2\Theta+\frac{\cos\mu^*\Theta}{\sin\mu^*\Theta}\mu^*\sin2\Theta=1-\mu^*\cos2\Theta+\frac{\cos\mu^*\Theta}{\sin\mu^*\Theta}[-\sin2\mu^*\Theta]\\&=1-\mu^*\cos2\Theta-2\cos^2\mu^*\Theta=-(\mu^*\cos2\Theta+\cos2\mu^*\Theta)=-\{\mu^*\cos2\Theta+\sqrt{1-(\mu^*\sin2\Theta)^2}\},\end{aligned} \tag{3.68}$$

where we have used (3.56) again. This completes the proof of (3.59) and (3.6). □

4. Models of crack singularity

In this section, let us consider the interior crack (i.e., crack tip) with free stress at $\theta=\pm\pi$. Since $\cos(n,x)=\pm\cos(\pi/2)=0$ and $\sin(n,x)=\pm\sin(\pi/2)=\pm1$, we have the boundary conditions from (3.35) and (3.36)

$$\sigma_{xy}=0,\quad \sigma_y=0\quad \text{at } \theta=\pm\pi. \tag{4.1}$$

Let $\Theta=\pi$, and free stress is assigned to the interior crack at $\theta=\pm\Theta(=\pm\pi)$. We may also choose a group of four coefficients a_k, b_k, c_k and d_k directly to satisfy the boundary conditions (4.1), to obtain the matrix equation

$$\mathbf{B}\mathbf{y}=\mathbf{0}, \tag{4.2}$$

where $\mathbf{y}=(a,b,c,d)^T$ and the matrix is given by

$$\mathbf{B}=\begin{pmatrix}D\mu^*(\mu^*-1)\cos(\mu^*-1)\pi & D\mu^*(\mu^*-1)\sin(\mu^*-1)\pi & \mu^*\cos(\mu^*-1)\pi & \mu^*\sin(\mu^*-1)\pi\\ -D\mu^*(\mu^*+1)\sin(\mu^*-1)\pi & D\mu^*(\mu^*+1)\cos(\mu^*-1)\pi & -\mu^*\sin(\mu^*-1)\pi & \mu^*\cos(\mu^*-1)\pi\\ D\mu^*(\mu^*-1)\cos(\mu^*-1)\pi & -D\mu^*(\mu^*-1)\sin(\mu^*-1)\pi & \mu^*\cos(\mu^*-1)\pi & -\mu^*\sin(\mu^*-1)\pi\\ D\mu^*(\mu^*+1)\sin(\mu^*-1)\pi & D\mu^*(\mu^*+1)\cos(\mu^*-1)\pi & \mu^*\sin(\mu^*-1)\pi & \mu^*\cos(\mu^*-1)\pi\end{pmatrix}. \tag{4.3}$$

When $\mu^*=n+\frac{1}{2}$, Eq. (4.3) leads to

$$\begin{pmatrix}0 & D\mu^*(\mu^*-1)\sin(\mu^*-1)\pi & 0 & \mu^*\sin(\mu^*-1)\pi\\ -D\mu^*(\mu^*+1)\sin(\mu^*-1)\pi & 0 & -\mu^*\sin(\mu^*-1)\pi & 0\\ 0 & -D\mu^*(\mu^*-1)\sin(\mu^*-1)\pi & 0 & -\mu^*\sin(\mu^*-1)\pi\\ D\mu^*(\mu^*+1)\sin(\mu^*-1)\pi & 0 & \mu^*\sin(\mu^*-1)\pi & 0\end{pmatrix}, \tag{4.4}$$

to give

$$c=-(n+\tfrac{3}{2})Da,\quad d=-(n-\tfrac{1}{2})Db\quad \text{for } \mu^*=n+\tfrac{1}{2}. \tag{4.5}$$

Next when $\mu^*=n$, Eq. (4.3) leads to

$$\begin{pmatrix}D\mu^*(\mu^*-1)\cos(\mu^*-1)\pi & 0 & \mu^*\cos(\mu^*-1)\pi & 0\\ 0 & D\mu^*(\mu^*+1)\cos(\mu^*-1)\pi & 0 & \mu^*\cos(\mu^*-1)\pi\\ D\mu^*(\mu^*-1)\cos(\mu^*-1)\pi & 0 & \mu^*\cos(\mu^*-1)\pi & 0\\ 0 & D\mu^*(\mu^*+1)\cos(\mu^*-1)\pi & 0 & \mu^*\cos(\mu^*-1)\pi\end{pmatrix}, \tag{4.6}$$

to give

$$c=-(n-1)Da,\quad d=-(n+1)Db\quad \text{for } \mu^*=n. \tag{4.7}$$

Q6 Hence Eqs. (2.30) and (2.31) are simplified as

$$u_L=\sum_{n=0}^{L-1}r^{n+1/2}\left\{a_{2n+1}\left[-\left(1+\left(n+\frac{3}{2}\right)D\right)\sin\left(n+\frac{1}{2}\right)\theta+D\left(n+\frac{1}{2}\right)\sin\left(n-\frac{3}{2}\right)\theta\right]+b_{2n+1}\left[\left(1+\left(n-\frac{1}{2}\right)D\right)\cos\left(n+\frac{1}{2}\right)\theta-D\left(n+\frac{1}{2}\right)\cos\left(n-\frac{3}{2}\right)\theta\right]\right\}+\sum_{n=1}^{L}r^n\{a_{2n}[-(1+(n-1)D)\sin n\theta+Dn\sin(n-2)\theta]+b_{2n}[(1+(n+1)D)\cos n\theta-Dn\cos(n-2)\theta]\}+b_0 \tag{4.8}$$

Please cite this article as: Lee M-G, et al. Combined Trefftz methods of particular and fundamental solutions for corner and crack singularity of linear elastostatics. Eng Anal Bound Elem (2010), doi:10.1016/j.enganabound.2010.02.005

$$v_L = \sum_{n=0}^{L-1} r^{n+1/2}\left\{a_{2n+1}\left[\left(1-\left(n+\frac{3}{2}\right)D\right)\cos\left(n+\frac{1}{2}\right)\theta + D\left(n+\frac{1}{2}\right)\cos\left(n-\frac{3}{2}\right)\theta\right] + b_{2n+1}\left[\left(1-\left(n-\frac{1}{2}\right)D\right)\sin\left(n+\frac{1}{2}\right)\theta + D\left(n+\frac{1}{2}\right)\sin\left(n-\frac{3}{2}\right)\theta\right]\right\} + \sum_{n=1}^{L} r^n\{a_{2n}[(1-(n-1)D)\cos n\theta + Dn\cos(n-2)\theta] + b_{2n}[(1-(n+1)D)\sin n\theta + Dn\sin(n-2)\theta]\} + a_0. \tag{4.9}$$

4.1. Symmetric Model C of crack singularity

Let us mimic the cracked-beam problem in [51] satisfying the boundary conditions in Fig. 1 for elastostatics. For the rectangle $S=\{(x,y)|-1\le x\le 1, 0\le y\le 1\}$, consider the free stress conditions on an interior crack at $\overline{OD}$, and the symmetric boundary conditions on $\overline{OA}\cup\overline{AB}\cup\overline{CD}$. We suppose that $v=1$ on $\overline{BC}$ and no exterior force along the x direction, which implies $\sigma_{xy}=u_y+v_x=0$. *Since* $v_x=0$ *on* $\overline{BC}$ *we have* $u_y = 0$. Then the symmetric model is given by $v=u_y=0$ at $\theta=0$. Since $\partial u/\partial y=\partial u/r\partial\theta=0$ at $\theta=0$, we have from (4.8) and $D\in(0,1)$

$$a_{2n+1}=a_{2n}=0. \tag{4.10}$$

Then Eq. (4.8) leads to

$$u_L = \sum_{n=0}^{L-1}\left\{r^{n+1/2}\left\{b_{2n+1}\left[\left(1+\left(n-\frac{1}{2}\right)D\right)\cos\left(n+\frac{1}{2}\right)\theta - D\left(n+\frac{1}{2}\right)\cos\left(n-\frac{3}{2}\right)\theta\right]\right\}\right\} + \sum_{n=1}^{L} r^n\{b_{2n}[(1+(n+1)D)\cos n\,\theta - Dn\cos(n-2)\theta]\} + b_0. \tag{4.11}$$

Also from $v=0$ at $\theta=0$ we also have (4.10), and then Eq. (4.9) leads to

$$v_L = \sum_{n=0}^{L-1} r^{n+1/2}\left\{b_{2n+1}\left[\left(1-\left(n-\frac{1}{2}\right)D\right)\sin\left(n+\frac{1}{2}\right)\theta + D\left(n+\frac{1}{2}\right)\sin\left(n-\frac{3}{2}\right)\theta\right]\right\} + \sum_{n=1}^{L} r^n\{b_{2n}[(1-(n+1)D)\sin n\theta + Dn\sin(n-2)\theta]\}. \tag{4.12}$$

Note that Eqs. (4.11) and (4.12) are exactly the same as those in [43], derived by different approaches. Model C is the symmetric model to satisfy the Cauchy–Navier equation (2.5) with the following boundary conditions:

$$\sigma_{xy}=\sigma_y=0 \quad \text{on } \overline{OD}, \tag{4.13}$$

$$v=u_y=0 \quad \text{on } \overline{OA}, \tag{4.14}$$

$$u=v_x=0 \quad \text{on } \overline{AB}\cup\overline{CD}, \tag{4.15}$$

$$v=1, \quad u_y=0 \quad \text{on } \overline{BC}. \tag{4.16}$$

4.2. Anti-symmetric model D of crack singularity

For the anti-symmetric model with $u=v_y=0$ at $\theta=0$ on $\overline{OA}$, Model D of crack singularity is called. Since coefficients $b_i=0\ \forall i$, the particular solutions are obtained from (4.8) and (4.9)

$$u_L = \sum_{n=0}^{L-1}\left\{r^{n+1/2}\left\{a_{2n+1}\left[-\left(1+\left(n+\frac{3}{2}\right)D\right)\sin\left(n+\frac{1}{2}\right)\theta + D\left(n+\frac{1}{2}\right)\sin\left(n-\frac{3}{2}\right)\theta\right]\right\}\right\} + \sum_{n=1}^{L} r^n\{a_{2n}[-(1+(n-1)D)\sin n\theta + Dn\sin(n-2)\theta]\}, \tag{4.17}$$

$$v_L = \sum_{n=0}^{L-1} r^{n+1/2}\left\{a_{2n+1}\left[\left(1-\left(n+\frac{3}{2}\right)D\right)\cos\left(n+\frac{1}{2}\right)\theta + D\left(n+\frac{1}{2}\right)\cos\left(n-\frac{3}{2}\right)\theta\right]\right\} + \sum_{n=1}^{L} r^n\{a_{2n}[(1-(n-1)D)\cos n\theta + Dn\cos(n-2)\theta]\} + a_0. \tag{4.18}$$

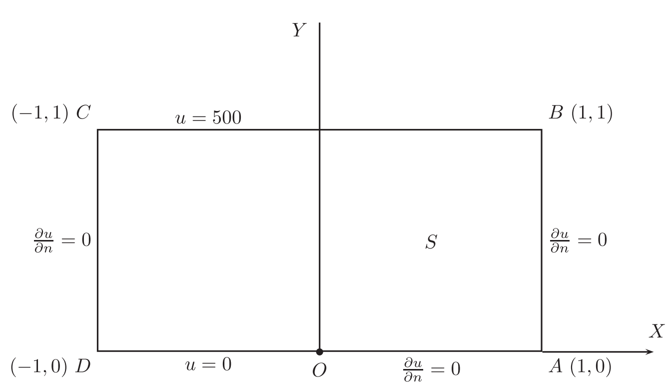

Fig. 1. The cracked-beam problem.

Please cite this article as: Lee M-G, et al. Combined Trefftz methods of particular and fundamental solutions for corner and crack singularity of linear elastostatics. Eng Anal Bound Elem (2010), doi:10.1016/j.enganabound.2010.02.005

Other boundary conditions are exactly the same as (4.13)–(4.16) in Model C. Note that Eqs. (4.17) and (4.18) and Model D are new, compared with [43].

4.3. Equivalence to the complex solutions in Piltner [55]

In Piltner [55], the explicit complex solutions at the crack tip (i.e., $\Theta=\pi$) with the free traction boundary are provided by (also see Domingues et al. [14]),

$$2\mu(u+iv)=\lambda\phi(z)-z\overline{\phi'(z)}-\overline{w(z)}, \tag{4.19}$$

where the complex variable

$$z=x+iy=re^{i\theta}=r(\cos\theta+i\sin\theta), \tag{4.20}$$

$r=\sqrt{x^2+y^2}$ and $\tan\theta=y/x$. The functions (4.19) are given by [14,55]

$$\phi(z)=\sum_{k=0}^{\infty}\gamma_k z^{k/2}, \tag{4.21}$$

$$w(z)=-\sum_{k=0}^{\infty}\left[\frac{k}{2}\gamma_k+\overline{\gamma}_k(-1)^k\right]z^{k/2}, \tag{4.22}$$

where the complex coefficients $\gamma_k=\alpha_k+i\beta_k$. Then we have from (4.19)

$$u=\frac{1}{2\mu}\Re\{\lambda\phi(z)-z\overline{\phi'(z)}-\overline{w(z)}\}, \tag{4.23}$$

$$v=\frac{1}{2\mu}\Im\{\lambda\phi(z)-z\overline{\phi'(z)}-\overline{w(z)}\}. \tag{4.24}$$

In the following, we will prove that the particular solutions of u and v from (4.23) and (4.24) are exactly the same as those in (4.8) and (4.9) by letting the constant $D=1/\lambda$.

First, we have from (4.20)

$$\gamma_k z^{k/2}=r^{k/2}(\alpha_k+i\beta_k)\left(\cos\frac{k}{2}\theta+i\sin\frac{k}{2}\theta\right)=r^{k/2}\left\{\alpha_k\cos\frac{k}{2}\theta-\beta_k\sin\frac{k}{2}\theta+i\left[\alpha_k\sin\frac{k}{2}\theta+\beta_k\cos\frac{k}{2}\theta\right]\right\}, \tag{4.25}$$

and from (4.21)

$$z\overline{\phi'(z)}=\sum_{k=0}^{\infty}\frac{k}{2}z\overline{\gamma_k z^{k/2-1}}=\sum_{k=0}^{\infty}\frac{k}{2}r^{k/2}\overline{(\alpha_k+i\beta_k)e^{i(k/2-2)\theta}}=\sum_{k=0}^{\infty}\frac{k}{2}r^{k/2}\left\{\alpha_k\cos\left(\frac{k}{2}-2\right)\theta-\beta_k\sin\left(\frac{k}{2}-2\right)\theta-i\left[\alpha_k\sin\left(\frac{k}{2}-2\right)\theta+\beta_k\cos\left(\frac{k}{2}-2\right)\theta\right]\right\}. \tag{4.26}$$

From (4.25) and (4.26) we have

$$\begin{aligned}\lambda\phi(z)-z\overline{\phi'(z)}&=\sum_{k=0}^{\infty}\left(\lambda\gamma_k z^{k/2}-\frac{k}{2}z\overline{\gamma}_k\overline{z}^{k/2-1}\right)=\sum_{k=0}^{\infty}r^{k/2}\left\{\alpha_k\left[\lambda\cos\frac{k}{2}\theta-\frac{k}{2}\cos\left(\frac{k}{2}-2\right)\theta\right]-\beta_k\left[\lambda\sin\frac{k}{2}\theta-\frac{k}{2}\sin\left(\frac{k}{2}-2\right)\theta\right]\right.\\&\quad\left.+i\left(\alpha_k\left[\lambda\sin\frac{k}{2}\theta+\frac{k}{2}\sin\left(\frac{k}{2}-2\right)\theta\right]+\beta_k\left[\lambda\cos\frac{k}{2}\theta+\frac{k}{2}\cos\left(\frac{k}{2}-2\right)\theta\right]\right)\right\}.\end{aligned} \tag{4.27}$$

Next, from (4.22) and (4.25) we have

$$\begin{aligned}-w(z)&=\sum_{k=0}^{\infty}\left[\frac{k}{2}(\alpha_k+i\beta_k)+(-1)^k(\alpha_k-i\beta_k)\right]r^{k/2}\left(\cos\frac{k}{2}\theta+i\sin\frac{k}{2}\theta\right)=\sum_{k=0}^{\infty}r^{k/2}\left[\left(\frac{k}{2}+(-1)^k\right)\alpha_k+i\left(\frac{k}{2}-(-1)^k\right)\beta_k\right]\left(\cos\frac{k}{2}\theta+i\sin\frac{k}{2}\theta\right)\\&=\sum_{k=0}^{\infty}r^{k/2}\left\{\alpha_k\left(\frac{k}{2}+(-1)^{k/2}\right)\cos\frac{k}{2}\theta-\beta_k\left(\frac{k}{2}-(-1)^k\right)\sin\frac{k}{2}\theta+i\left[\alpha_k\left(\frac{k}{2}+(-1)^k\right)\sin\frac{k}{2}\theta+\beta_k\left(\frac{k}{2}-(-1)^k\right)\cos\frac{k}{2}\theta\right]\right\}.\end{aligned} \tag{4.28}$$

Combining (4.19), (4.27) and (4.28) gives

$$\begin{aligned}\lambda\phi(z)-z\overline{\phi'(z)}-\overline{w(z)}&=\sum_{k=0}^{\infty}r^{k/2}\left\{\alpha_k\left[\lambda\cos\frac{k}{2}\theta-\frac{k}{2}\cos\left(\frac{k}{2}-2\right)\theta+\left(\frac{k}{2}+(-1)^k\right)\cos\frac{k}{2}\theta\right]-\beta_k\left[\lambda\sin\frac{k}{2}\theta-\frac{k}{2}\sin\left(\frac{k}{2}-2\right)\theta+\left(\frac{k}{2}-(-1)^k\right)\sin\frac{k}{2}\theta\right]\right.\\&\quad\left.+i\left(\alpha_k\left[\lambda\sin\frac{k}{2}\theta+\frac{k}{2}\sin\left(\frac{k}{2}-2\right)\theta-\left(\frac{k}{2}+(-1)^k\right)\sin\frac{k}{2}\theta\right]+\beta_k\left[\lambda\cos\frac{k}{2}\theta+\frac{k}{2}\cos\left(\frac{k}{2}-2\right)\theta-\left(\frac{k}{2}-(-1)^k\right)\cos\frac{k}{2}\theta\right]\right)\right\}.\end{aligned} \tag{4.29}$$

Please cite this article as: Lee M-G, et al. Combined Trefftz methods of particular and fundamental solutions for corner and crack singularity of linear elastostatics. Eng Anal Bound Elem (2010), doi:10.1016/j.enganabound.2010.02.005

Hence we have from (4.23), (4.24) and (4.29)

$$u=\frac{1}{2\mu}\sum_{k=0}^{\infty}r^{k/2}\left\{\alpha_k\left[\lambda\cos\frac{k}{2}\theta-\frac{k}{2}\cos\left(\frac{k}{2}-2\right)\theta+\left(\frac{k}{2}+(-1)^k\right)\cos\frac{k}{2}\theta\right]-\beta_k\left[\lambda\sin\frac{k}{2}\theta-\frac{k}{2}\sin\left(\frac{k}{2}-2\right)\theta+\left(\frac{k}{2}-(-1)^k\right)\sin\frac{k}{2}\theta\right]\right\}, \tag{4.30}$$

$$v=\frac{1}{2\mu}\sum_{k=0}^{\infty}r^{k/2}\left\{\alpha_k\left[\lambda\sin\frac{k}{2}\theta+\frac{k}{2}\sin\left(\frac{k}{2}-2\right)\theta-\left(\frac{k}{2}+(-1)^k\right)\sin\frac{k}{2}\theta\right]+\beta_k\left[\lambda\cos\frac{k}{2}\theta+\frac{k}{2}\cos\left(\frac{k}{2}-2\right)\theta-\left(\frac{k}{2}-(-1)^k\right)\cos\frac{k}{2}\theta\right]\right\}. \tag{4.31}$$

Since $D=1/\lambda$, for $k=2n$ and $k=2n+1$ we have from (4.30)

$$u=\frac{1}{2\mu D}\left\{\sum_{k=0}^{\infty}r^{n+1/2}\alpha_{2n+1}\left[\cos\left(n+\frac{1}{2}\right)\theta-D\left(n+\frac{1}{2}\right)\cos\left(n-\frac{3}{2}\right)\theta+D\left(n-\frac{1}{2}\right)\cos\left(n+\frac{1}{2}\right)\theta\right]+\sum_{k=1}^{\infty}r^{n}\alpha_{2n}[\cos n\theta-Dn\cos(n-2)\theta+D(n+1)\cos n\theta]\right.$$
$$\left.-\sum_{k=0}^{\infty}r^{n+1/2}\beta_{2n+1}\left[\sin\left(n+\frac{1}{2}\right)\theta-D\left(n+\frac{1}{2}\right)\sin\left(n-\frac{3}{2}\right)\theta+D\left(n+\frac{3}{2}\right)\sin\left(n+\frac{1}{2}\right)\theta\right]-\sum_{k=1}^{\infty}r^{n}\beta_{2n}[\sin n\theta-Dn\sin(n-2)\theta+D(n-1)\sin n\theta]\right\}. \tag{4.32}$$

Also from (4.31),

$$v=\frac{1}{2\mu D}\left\{\sum_{k=0}^{\infty}r^{n+1/2}\alpha_{2n+1}\left[\sin\left(n+\frac{1}{2}\right)\theta+D\left(n+\frac{1}{2}\right)\sin\left(n-\frac{3}{2}\right)\theta-D\left(n-\frac{1}{2}\right)\sin\left(n+\frac{1}{2}\right)\theta\right]+\sum_{k=1}^{\infty}r^{n}\alpha_{2n}[\sin n\theta+Dn\sin(n-2)\theta-D(n+1)\sin n\theta]\right.$$
$$\left.+\sum_{k=0}^{\infty}r^{n+1/2}\beta_{2n+1}\left[\cos\left(n+\frac{1}{2}\right)\theta+D\left(n+\frac{1}{2}\right)\cos\left(n-\frac{3}{2}\right)\theta-D\left(n+\frac{3}{2}\right)\cos\left(n+\frac{1}{2}\right)\theta\right]+\sum_{k=1}^{\infty}r^{n}\beta_{2n}[\cos n\theta+Dn\cos(n-2)\theta-D(n-1)\cos n\theta]\right\}. \tag{4.33}$$

By letting

$$b_n=\frac{\alpha_n}{2\mu D},\quad a_n=\frac{\beta_n}{2\mu D},$$

Eqs. (4.32) and (4.33) lead to the exact particular solutions (4.8) and (4.9). This completes the proof of the equivalence between the explicit complex solutions in [55] and the explicit particular solutions for the crack tip with the free traction conditions. Note that by our systematic analysis, the explicit particular solutions (4.8) and (4.9) are easily derived, and their simple functions can be applied widely for practical problems.

5. The collocation Trefftz method

Take Model C as example. We choose the particular solutions (4.11) and (4.12), and denote this solution set by V_L. Since they satisfy the governed equations (2.5) and the boundary conditions on $\overline{OD}\cup\overline{OA}$ in Fig. 1 already, the coefficients a_k and b_k are sought by satisfying the rest of boundary conditions in (4.15) and (4.16). Define the boundary energy

$$I(u,v)=\int_{\overline{BC}}[(v-1)^2+w^2u_y^2]+\int_{\overline{AB}\cup\overline{CD}}[u^2+w^2v_x^2], \tag{5.1}$$

where w is a weight. We choose $w=1/L$ in computation. The collocation Trefftz method (CTM) reads: To seek $(u_N,v_N)\in V_L$ such that

$$I(u_L,v_L)=\min_{(u,v)\in V_L}I(u,v). \tag{5.2}$$

When the integrals in (5.1) involve integration approximation, the numerical solutions are given by

$$\hat{I}(u_L,v_L)=\min_{(u,v)\in V_L}\hat{I}(u,v), \tag{5.3}$$

where

$$\hat{I}(u,v)=\hat{\int}_{\overline{BC}}[(v-1)^2+w^2u_y^2]+\hat{\int}_{\overline{AB}\cup\overline{CD}}[u^2+w^2v_x^2], \tag{5.4}$$

where $\hat{\int}$ is the numerical approximation of $\int$ by some rules, such as the central or the Gauss rule.

We may establish the collocation equations of u_L and v_L, to satisfy (4.15) and (4.16) directly. Denote the basis of particular solutions by

$$\Phi_{2n+1}(r,\theta)=r^{n+1/2}\left[\left(1+D\left(n-\frac{1}{2}\right)\right)\cos\left(n+\frac{1}{2}\right)\theta-D\left(n+\frac{1}{2}\right)\cos\left(n-\frac{3}{2}\right)\theta\right],\quad \Phi_{2n}(r,\theta)=r^n[(1+(n+1)D)\cos n\theta-Dn\cos(n-2)\theta], \tag{5.5}$$

$$\Psi_{2n+1}(r,\theta)=r^{n+1/2}\left[\left(1-\left(n-\frac{1}{2}\right)D\right)\sin\left(n+\frac{1}{2}\right)\theta+D\left(n+\frac{1}{2}\right)\sin\left(n-\frac{3}{2}\right)\theta\right],\quad \Psi_{2n}(r,\theta)=r^n[(1-(n+1)D)\sin n\theta+Dn\sin(n-2)\theta]. \tag{5.6}$$

Then the solutions (4.11) and (4.12) are denoted simply by

$$u_L=\sum_{n=1}^{2L}b_n\Phi_n(r,\theta)+b_0,\quad v_L=\sum_{n=1}^{2L}b_n\Psi_n(r,\theta). \tag{5.7}$$

Let $\overline{AB} \cup \overline{BC} \cup \overline{CD}$ be divided uniformly into small sections with length $h(=1/N)$. On $\overline{BC}$, let $Q_i=(r_i,\theta_i)$ denote the middle nodes of the small sections, we may have the following collocation equations from (4.16)

$$\sqrt{h}\left\{\sum_{n=1}^{2L} b_n \Psi_n(r_i,\theta_i)\right\}=\sqrt{h}, \quad (r_i,\theta_i)\in \overline{BC}, \tag{5.8}$$

$$w\sqrt{h}\sum_{n=1}^{2L} b_n \frac{\partial}{\partial y}\Phi_n(r_i,\theta_i)=0, \quad (r_i,\theta_i)\in \overline{BC}, \tag{5.9}$$

where w is a weight constant to balance two kinds of collocation equations. In computation, we choose $w=1/L$ (see [38]). Similarly, from (4.15), we obtain the collocation equations on $\overline{AB}\cup\overline{CD}$,

$$\sqrt{h}\left\{\sum_{n=1}^{2L} b_n \Phi_n(r_i,\theta_i)+b_0\right\}=0, \quad (r_i,\theta_i)\in \overline{AB}\cup\overline{CD}, \tag{5.10}$$

$$w\sqrt{h}\sum_{n=1}^{2L} b_n \frac{\partial}{\partial x}\Psi_n(r_i,\theta_i)=0, \quad (r_i,\theta_i)\in \overline{AB}\cup\overline{CD}. \tag{5.11}$$

Eqs. (5.8)–(5.11) form the linear algebraic equations,

$$\mathbf{F}\mathbf{x}=\mathbf{b}, \tag{5.12}$$

where $\mathbf{F}\in R^{m\times n}(m\ge n)$, $\mathbf{x}\in R^n$ and $\mathbf{b}\in R^m$. The number of unknown coefficients is $n = 2L+1$ and $m = 8M$ and M denotes the number of collocation nodes on $\overline{AB}$. In computation, we always choose $m>n$. Hence Eq. (5.12) is the system of over-determined equations. We may choose the least squares method, or the QR factorization, to seek the coefficient vector $\mathbf{x}=\{b_0,b_1,b_2,\ldots,b_{2L}\}^T$. The CTM is studied in [44] for Poisson's, biharmonic and Helmholtz equations, as well as eigenvalue problems. The equivalence between (5.3) and the above collocation equations (5.12) can be proven easily by the following [44]. Error bounds may also be derived; details appear elsewhere.

To measure numerical stability, we compute the condition number for (5.12) by

$$\mathrm{Cond}=\frac{\sigma_{max}}{\sigma_{min}}, \tag{5.13}$$

where σ_{max} and σ_{min} are the maximal and the minimal singular values of matrix $\mathbf{F}$, respectively. A better criterion of numerical stability is given by the effective condition number in Li et al. [42], defined by

$$\mathrm{Cond\_eff}=\frac{\|\mathbf{b}\|}{\sigma_{min}\|\mathbf{x}\|}, \tag{5.14}$$

where $\|\mathbf{x}\|$ and $\|\mathbf{b}\|$ are the 2-norms.

6. Fundamental solutions

The fundamental solutions (FS) are important for linear elastostatics in both theory and computation. Although the FS are used in many papers of linear elastostatics, there seems to be a lack of systematic analysis of the explicit functions and their applications for singularity problems. The systematic analysis of the FS is one of goals of this paper, and it is explored in the rest of this paper.

Let $\vec{d}_i=(a_i,b_i)^T$ with the constants a_i and b_i, and $\vec{w}_i=(u_i,v_i)^T$, we have from the principal fundamental solutions in Chen and Zhou [7]

$$\vec{w}_i=E_2(\mathbf{x},\xi_i)\vec{d}_i, \tag{6.1}$$

where

$$E_2(\mathbf{x},\xi)=\frac{\lambda+3\mu}{4\pi\mu(\lambda+2\mu)}\left\{-\ln r_{\mathbf{x}\xi}I_2+\frac{\lambda+\mu}{\lambda+3\mu}\frac{1}{r_{\mathbf{x}\xi}^2}[(\mathbf{x}-\xi)(\mathbf{x}-\xi)^T]\right\}, \tag{6.2}$$

where $r_{\mathbf{x}\xi}=|\mathbf{x}-\xi|$ and I_2 is the identity matrix. Choose the source points $Q=\vec{\xi}_i=(\xi_i,\eta_i)$ to be uniformly located on the larger circle ℓ_R of the solution domain S, based on Bogomolny [4] and Li [40]. We have

$$x=r\cos\theta, \quad y=r\sin\theta,$$

$$\xi_i=R\cos\phi_i, \quad \eta_i=R\sin\phi_i, \quad i=1,2,\ldots,n, \tag{6.3}$$

where the radius of ℓ_R is $R>\max_S r$. For the uniform source nodes, $r=\sqrt{x^2+y^2}$, $R=\sqrt{\xi_i^2+\eta_i^2}$ and $\phi_i=i2\pi/N$, we have

$$r_i=r_{\mathbf{x}\xi}=r(\mathbf{x}\vec{\xi}_{\mathbf{i}})=\sqrt{R^2+r^2-2Rr\cos(\theta-\phi_i)}. \tag{6.4}$$

Then the principal fundamental solutions are given by

$$\vec{w}_i=E_2(\mathbf{x},\xi_i)\vec{d}_i, \quad i=1,2,\ldots,n, \tag{6.5}$$

where

$$u_i=a_i\left(-A\ln r_i+B\frac{(x-\xi_i)^2}{r_i^2}\right)+b_iB\frac{(x-\xi_i)(y-\eta_i)}{r_i^2}, \tag{6.6}$$

$$v_i = a_i B \frac{(x-\xi_i)(y-\eta_i)}{r_i^2} + b_i\left(-A\ln r_i + B\frac{(y-\eta_i)^2}{r_i^2}\right), \tag{6.7}$$

and the constants

$$A = \frac{\lambda+3\mu}{4\pi\mu(\lambda+2\mu)}, \quad B = \frac{\lambda+\mu}{4\pi\mu(\lambda+2\mu)}. \tag{6.8}$$

By adding the fundamental solutions $\nabla(-\ln r_i)$ in (2.14), we obtain linear combination of all fundamental solutions,

$$u_N = u_N(x,y) = \sum_{i=1}^{N}\left\{a_i\left(-\ln r_i + D\frac{(x-\xi_i)^2}{r_i^2}\right) + b_i D\frac{(x-\xi_i)(y-\eta_i)}{r_i^2} + c_i\frac{(x-\xi_i)}{r_i^2}\right\}, \tag{6.9}$$

$$v_N = v_N(x,y) = \sum_{i=1}^{N}\left\{a_i D\frac{(x-\xi_i)(y-\eta_i)}{r_i^2} + b_i\left(-\ln r_i + D\frac{(y-\eta_i)^2}{r_i^2}\right) + c_i\frac{(y-\eta_i)}{r_i^2}\right\}, \tag{6.10}$$

where a_i, b_i and c_i are the coefficients, the constant

$$D = \frac{B}{A} = \frac{\kappa}{1-\kappa} = \frac{\lambda+\mu}{\lambda+3\mu} = \frac{1}{3-4v}, \tag{6.11}$$

for the plan strain problems, and κ is given in (2.11).

6.1. Equivalence to complex FS

The complex fundamental solutions (CFS) are given in [52,31]. Denote the complex function $w_N^*(x,y) = u_N(x,y) + iv_N(x,y)$ and the complex coefficients $\alpha_j = a_j + ib_j$. Let $\vec{P} = (x,y)^T$ and $\vec{Q}_j = (\xi_j,\eta_j)^T$. The CFS are given by

$$w_N^*(Q_j,P) = \sum_{j=1}^{N}\left\{\ln(z_{Q_j}-z_P)(\overline{z}_{Q_j}-\overline{z}_P)\alpha_j + D\frac{(z_{Q_j}-z_P)}{(\overline{z}_{Q_j}-\overline{z}_P)}\overline{\alpha}_j\right\}, \tag{6.12}$$

where D is given in (6.11). There exists the equality,

$$\frac{z}{\overline{z}} = \frac{x+iy}{x-iy} = \frac{x^2-y^2}{r^2} + i\frac{2xy}{r^2}, \tag{6.13}$$

where $r = \sqrt{x^2+y^2}$. We obtain from (6.12) and (6.13)

$$u_N(x,y) = \sum_{j=1}^{N}\left\{a_j\left(-2\ln r_{PQ_j} + D\frac{1}{r_{PQ_j}^2}[(x-\xi_j)^2-(y-\eta_j)^2]\right) + b_j 2D\frac{(x-\xi_j)(y-\eta_j)}{r_{PQ_j}^2}\right\}, \tag{6.14}$$

$$v_N(x,y) = \sum_{j=1}^{N}\left\{b_j\left(-2\ln r_{PQ_j} + D\frac{1}{r_{PQ_j}^2}[(y-\eta_j)^2-(x-\xi_j)^2]\right) + a_j 2D\frac{(x-\xi_j)(y-\eta_j)}{r_{PQ_j}^2}\right\}, \tag{6.15}$$

where $r_{PQ_j} = \sqrt{(x-\xi_j)^2+(y-\eta_j)^2}$. By using the relations,

$$\frac{1}{r_{PQ_j}^2}[(x-\xi_j)^2-(y-\eta_j)^2] = 2\frac{(x-\xi_j)^2}{r_{PQ_j}^2} - 1,$$

$$\frac{1}{r_{PQ_j}^2}[(y-\eta_j)^2-(x-\xi_j)^2] = 2\frac{(y-\eta_j)^2}{r_{PQ_j}^2} - 1, \tag{6.16}$$

Eqs. (6.14) and (6.15) lead to

$$u_N(x,y) = 2\sum_{j=1}^{N}\left\{a_j\left(-\ln r_{PQ_j} + D\left[\frac{(x-\xi_j)^2}{r_{PQ_j}^2} - \frac{1}{2}\right]\right) + b_j D\frac{(x-\xi_j)(y-\eta_j)}{r_{PQ_j}^2}\right\}, \tag{6.17}$$

$$v_N(x,y) = 2\sum_{j=1}^{N}\left\{b_j\left(-\ln r_{PQ_j} + D\left[\frac{(y-\eta_j)^2}{r_{PQ_j}^2} - \frac{1}{2}\right]\right) + a_j D\frac{(x-\xi_j)(y-\eta_j)}{r_{PQ_j}^2}\right\}. \tag{6.18}$$

Comparing (6.17) and (6.18) with (6.9) and (6.10), there is a difference of translation. Hence, the equivalence of the FS and the CFS is proved.

6.2. Proof of fundamental solutions

First let $\vec{h} \equiv 0$, and then $q = -\ln r$, we have the simple FS from (2.14)

$$\vec{w}(\vec{x}) = -\kappa\nabla q = -\kappa(q_x,q_y)^T = \kappa\left(\frac{x}{r^2},\frac{y}{r^2}\right)^T. \tag{6.19}$$

Please cite this article as: Lee M-G, et al. Combined Trefftz methods of particular and fundamental solutions for corner and crack singularity of linear elastostatics. Eng Anal Bound Elem (2010), doi:10.1016/j.enganabound.2010.02.005

We may verify the FS in (6.19) satisfying (2.5). Since $\Delta q = \Delta(-\ln r) = 0$, we have

$$\nabla \cdot \vec{w} = -\kappa(q_{xx} + q_{yy}) = -\kappa \Delta q = 0,$$

$$\nabla(\nabla \cdot \vec{w}) = \nabla(-\kappa \Delta q) = 0,$$

$$\Delta \vec{w} = -\kappa \Delta (q_x, q_y)^T = -\kappa\{(\Delta q)_x, (\Delta q)_y\}^T = (0,0)^T. \tag{6.20}$$

Evidently, Eq. (2.5) is satisfied.

Next, let $q = 0$, we have the principal FS from (2.14)

$$\vec{w}(\vec{x}) = \vec{h}(\vec{x}) - \kappa \nabla[\vec{x} \cdot \vec{h}(\vec{x})]. \tag{6.21}$$

The FS in (6.2) is expressed simply in the matrix form with a constant factor difference

$$\begin{pmatrix} -\ln r(1-\kappa) + \kappa \dfrac{x^2}{r^2} & \kappa \dfrac{xy}{r^2} \\ \kappa \dfrac{xy}{r^2} & -\ln r(1-\kappa) + \kappa \dfrac{y^2}{r^2} \end{pmatrix} = (1-\kappa) \begin{pmatrix} -\ln r + D\dfrac{x^2}{r^2} & D\dfrac{xy}{r^2} \\ D\dfrac{xy}{r^2} & -\ln r + D\dfrac{y^2}{r^2} \end{pmatrix}, \tag{6.22}$$

where D is given in (6.11). Below we will derive (6.22) directly from (6.21).

Let $\vec{h}(\mathbf{x}) = (-\ln r, 0)^T$, where $r = \sqrt{x^2+y^2}$. We have

$$\vec{w}^*(\mathbf{x}) = \begin{pmatrix} -\ln r \\ 0 \end{pmatrix} + \kappa \begin{pmatrix} \dfrac{\partial}{\partial x}(x \ln r) \\ \dfrac{\partial}{\partial y}(x \ln r) \end{pmatrix}. \tag{6.23}$$

Since there are the derivatives

$$\frac{\partial}{\partial x}(x \ln r) = \ln r + \frac{x^2}{r^2}, \quad \frac{\partial}{\partial y}(x \ln r) = \frac{xy}{r^2}, \tag{6.24}$$

we obtain from (6.23)

$$\vec{w}^*(\mathbf{x}) = \begin{pmatrix} -\ln r(1-\kappa) + \kappa \dfrac{x^2}{r^2} \\ \kappa \dfrac{xy}{r^2} \end{pmatrix}. \tag{6.25}$$

Next choose $\vec{h}(\mathbf{x}) = (0, -\ln r)^T$, we have

$$\vec{w}^*(\mathbf{x}) = \begin{pmatrix} 0 \\ -\ln r \end{pmatrix} + \kappa \begin{pmatrix} \dfrac{\partial}{\partial x}(y \ln r) \\ \dfrac{\partial}{\partial y}(y \ln r) \end{pmatrix} = \begin{pmatrix} \kappa \dfrac{xy}{r^2} \\ -\ln r(1-\kappa) + \kappa \dfrac{y^2}{r^2} \end{pmatrix}. \tag{6.26}$$

Combining (6.25) and (6.26) gives the desired matrix (6.22).

Below we prove the principal FS in (6.22) also satisfy the Cauchy–Navier equation (2.5). First for $\vec{h}(\mathbf{x}) = (-\ln r, 0)^T$, from (6.25) we have

$$\nabla \cdot \vec{w}^*(\vec{x}) = \frac{\partial}{\partial x}\left[-\ln r(1-\kappa) + \kappa \frac{x^2}{r^2}\right] + \frac{\partial}{\partial y}\left(\kappa \frac{xy}{r^2}\right) = -(1-\kappa)\frac{x}{r^2} + 2\kappa \frac{x}{r^2} + \kappa x^2 \frac{\partial}{\partial x}\left(\frac{1}{r^2}\right) + \kappa \frac{x}{r^2} + \kappa xy \frac{\partial}{\partial y}\left(\frac{1}{r^2}\right). \tag{6.27}$$

Since

$$\frac{\partial}{\partial x}\left(\frac{1}{r^2}\right) = -\frac{2}{r^3}\frac{x}{r} = -2\frac{x}{r^4}, \quad \frac{\partial}{\partial y}\left(\frac{1}{r^2}\right) = -2\frac{y}{r^4}, \tag{6.28}$$

Eq. (6.27) leads to

$$\nabla \cdot \vec{w}^*(\vec{x}) = -\frac{x}{r^2} + 4\kappa \frac{x}{r^2} - 2\kappa \frac{x^3}{r^4} - 2\kappa \frac{xy^2}{r^4} = (-1+2\kappa)\frac{x}{r^2}, \tag{6.29}$$

where we have used the equality: $x^3/r^4 + xy^2/r^4 = x/r^2$. Next, consider the integral

$$\mu \iint_{B_\varepsilon} \left\{ \Delta \vec{w}^* + \frac{1}{1-2v} \nabla[\nabla \cdot \vec{w}^*] \right\}, \tag{6.30}$$

where B_ε is a disk with the origin center and the radius ε. From (6.29) we have

$$\nabla[\nabla \cdot \vec{w}^*] = (-1+2\kappa)\left(\frac{\partial}{\partial x}\frac{x}{r^2}, \frac{\partial}{\partial y}\frac{x}{r^2}\right)^T. \tag{6.31}$$

Hence we obtain from (6.25) and (6.30)

$$\vec{T} = (T_1, T_2)^T = \mu \iint_{B_\varepsilon} \begin{pmatrix} \Delta\left[-\ln r(1-\kappa) + \kappa \dfrac{x^2}{r^2}\right] + \dfrac{-1+2\kappa}{1-2v} \dfrac{\partial}{\partial x} \dfrac{x}{r^2} \\ \kappa \Delta\left(\dfrac{xy}{r^2}\right) + \dfrac{(-1+2\kappa)}{1-2v} \dfrac{\partial}{\partial y} \dfrac{x}{r^2} \end{pmatrix}. \tag{6.32}$$

Please cite this article as: Lee M-G, et al. Combined Trefftz methods of particular and fundamental solutions for corner and crack singularity of linear elastostatics. Eng Anal Bound Elem (2010), doi:10.1016/j.enganabound.2010.02.005

Let us check the first component of the above equation. From the Green formula, we have

$$T_1=\mu\iint_{B_\varepsilon}\Delta\left[-\ln r(1-\kappa)+\kappa\frac{x^2}{r^2}\right]+\frac{-1+2\kappa}{1-2\nu}\frac{\partial}{\partial x}\frac{x}{r^2}=\mu\int_{\partial B_\varepsilon}\left\{\frac{\partial}{\partial r}\left[-\ln r(1-\kappa)+\kappa\frac{x^2}{r^2}\right]+\frac{-1+2\kappa}{1-2\nu}\frac{x}{r^2}\cos(n,x)\right\}. \tag{6.33}$$

Denote $x=r\cos\theta$ and $y=r\sin\theta$. We have

$$\frac{\partial}{\partial r}\left[-\ln r(1-\kappa)+\kappa\frac{x^2}{r^2}\right]=\frac{\partial}{\partial r}\left[-\ln r(1-\kappa)+\kappa\frac{r^2\cos^2\theta}{r^2}\right]=-\frac{1}{r}(1-\kappa),$$

$$\frac{x}{r^2}\cos(n,x)=\frac{\cos^2\theta}{r}. \tag{6.34}$$

The component T_1 in (6.33) gives

$$T_1=\mu\int_0^{2\pi}r\,d\theta\left\{-\frac{1-\kappa}{r}+\frac{-1+2\kappa}{1-2\nu}\frac{\cos^2\theta}{r}\right\}=\mu 2\pi\left\{-(1-\kappa)+\frac{-1+2\kappa}{1-2\nu}\frac{1}{2}\right\}=-2\pi\mu+\pi\mu\left[2\kappa+\frac{-1+2\kappa}{1-2\nu}\right]=-2\pi\mu, \tag{6.35}$$

where we have used $2\kappa+(-1+2\kappa)/(1-2\nu)=0$ due to $\kappa=1/4(1-\nu)$.

Finally, for the second component T_2 in (6.32), we have

$$T_2=\mu\iint_{B_\varepsilon}\left\{\kappa\Delta\left(\frac{xy}{r^2}\right)+\frac{-1+2\kappa}{1-2\nu}\frac{\partial}{\partial y}\frac{x}{r^2}\right\}=\mu\int_{\partial B_\varepsilon}\left\{\kappa\frac{\partial}{\partial r}\left[\frac{r^2\cos\theta\sin\theta}{r^2}\right]+\frac{-1+2\kappa}{1-2\nu}\frac{x}{r^2}\sin\theta\right\}=\mu\frac{-1+2\kappa}{1-2\nu}\int_0^{2\pi}r\,d\theta\frac{r\cos\theta}{r^2}\sin\theta$$
$$=\mu\frac{-1+2\kappa}{1-2\nu}\int_0^{2\pi}\cos\theta\sin\theta\,d\theta=0. \tag{6.36}$$

From (6.35) and (6.36), the integral $\vec{T}$ in (6.30) leads to

$$\mu\iint_{B_\varepsilon}\left\{\Delta\vec{w}^*+\frac{1}{1-2\nu}\nabla[\nabla\cdot\vec{w}^*]\right\}=(-2\pi\mu,0)^T. \tag{6.37}$$

Similarly, for $\vec{h}(\mathbf{x})=(0,-\ln r)^T$, we can show

$$\mu\iint_{B_\varepsilon}\left\{\Delta\vec{w}^*+\frac{1}{1-2\nu}\nabla[\nabla\cdot\vec{w}^*]\right\}=(0,-2\pi\mu)^T. \tag{6.38}$$

Hence, by noting (6.1) we obtain the FS in (6.22) as

$$\vec{E}_2(\mathbf{x},\xi)=\frac{1-\kappa}{2\pi\mu}\begin{pmatrix}-\ln r_{\mathbf{x}\xi}+D\dfrac{(x-\xi)^2}{r^2_{\mathbf{x}\xi}} & D\dfrac{(x-\xi)(y-\eta)}{r^2_{\mathbf{x}\xi}}\\ D\dfrac{(x-\xi)(y-\eta)}{r^2_{\mathbf{x}\xi}} & -\ln r_{\mathbf{x}\xi}+D\dfrac{(y-\eta)^2}{r^2_{\mathbf{x}\xi}}\end{pmatrix}, \tag{6.39}$$

where $\mathbf{x}=(x,y)^T$, $\vec{\xi}=(\xi,\eta)^T$, $r_{\mathbf{x}\xi}=\sqrt{(x-\xi)^2+(y-\eta)^2}$ and $D=\kappa/(1-\kappa)$. The principal FS in (6.39) satisfy the governed equation (2.5).

Remark 6.1. This paper also provides a *systematic* analysis for the FS. The FS are derived in detail, and the proof is provided for the FS to satisfy the Cauchy–Navier equations (2.17) and (2.18) in 2D. Also an equivalence is proved for the FS in this paper and the complex FS in [52,31]. This section is devoted to smooth solutions, and the next section to singularity solutions.

7. The combined Trefftz method with many FS but a few singular PS

Since both the fundamental solutions (FS) and the particular solutions satisfy the Cauchy–Navier equations (2.4) and (2.5), they can be used as the admissible functions in the CTM, to seek numerical solutions. However, since the FS are smooth, the solutions by the MFS are poor for corner singularity problems. We may add a few singular (but not smooth) particular solutions given in (3.61) and (3.62), where the values of leading μ_k can be computed numerically in [43]. Note that the explicit particular solutions can be found only for the crack tip (i.e., $\Theta=\pi$). For general corners with $\Theta\neq\pi$, the powers ν_k satisfying (3.57) have to be computed first, see [43]. Choosing *a few* singular particular solutions will greatly simplify the numerical algorithms for the Cauchy–Navier equation with corners. Hence the combined Trefftz methods in this paper are more efficient and advantageous for numerical solutions of linear elastostatics with singularity.

In this section, we choose Models C and D, to give numerical algorithms first by using the particular solutions in (4.11) and (4.12), and then by the combined Trefftz methods with many FS and a few singular PS.

7.1. Combined algorithms

Take Model C for example. From (6.14) and (6.15), we choose the mixed type of FS and PS,

$$u_{N-L}(x,y)=\sum_{j=1}^{N}\left\{a_j\left(-2\ln r_{PQ_j}+D\frac{1}{r^2_{PQ_j}}[(x-\xi_j)^2-(y-\eta_j)^2]\right)+b_j 2D\frac{(x-\xi_j)(y-\eta_j)}{r^2_{PQ_j}}+c_j\frac{(x-\xi_j)}{r^2_{PQ_j}}\right\}+\sum_{j=1}^{L}d_{2j+1}\Phi_{2j+1}(r,\theta)+d_0, \tag{7.1}$$

$$v_{N-L}(x,y)=\sum_{j=0}^{N}\left\{b_j\left(-2\ln r_{PQ_j}+D\frac{1}{r^2_{PQ_j}}[(y-\eta_j)^2-(x-\xi_j)^2]\right)+a_j 2D\frac{(x-\xi_j)(y-\eta_j)}{r^2_{PQ_j}}+c_j\frac{(y-\eta_j)}{r^2_{PQ_j}}\right\}+\sum_{j=1}^{L}d_{2j+1}\Psi_{2j+1}(r,\theta), \tag{7.2}$$

where only the singular particular solutions $\Phi_{2j+1}(r,\theta)$ and $\Psi_{2j+1}(r,\theta)$ are selected from (5.5) and (5.6), and a_j, b_j,c_j, d_j are coefficients to be sought. Note that we do not need the smooth particular solution in (5.5) and (5.6), because the FS can approximate very well the smooth part of the solutions. In computation, we choose N and $L \le 4$ with the following singular particular solutions:

$$\Phi_1(r,\theta)=r^{1/2}\left[\left(1-\frac{D}{2}\right)\cos\frac{\theta}{2}-\frac{D}{2}\cos\left(\frac{3\theta}{2}\right)\right],\quad \Phi_3(r,\theta)=r^{3/2}\left[\left(1+\frac{D}{2}\right)\cos\frac{3\theta}{2}-\frac{3D}{2}\cos\left(\frac{\theta}{2}\right)\right],$$

$$\Phi_5(r,\theta)=r^{5/2}\left[\left(1+\frac{3D}{2}\right)\cos\frac{5\theta}{2}-\frac{5D}{2}\cos\left(\frac{\theta}{2}\right)\right],\quad \Phi_7(r,\theta)=r^{7/2}\left[\left(1+\frac{5D}{2}\right)\cos\frac{7\theta}{2}-\frac{7D}{2}\cos\left(\frac{3\theta}{2}\right)\right],$$

$$\Psi_1(r,\theta)=r^{1/2}\left[\left(1+\frac{D}{2}\right)\sin\frac{\theta}{2}-\frac{D}{2}\sin\left(\frac{3\theta}{2}\right)\right],\quad \Psi_3(r,\theta)=r^{3/2}\left[\left(1-\frac{D}{2}\right)\sin\frac{3\theta}{2}-\frac{3D}{2}\sin\left(\frac{\theta}{2}\right)\right],$$

$$\Psi_5(r,\theta)=r^{5/2}\left[\left(1-\frac{3D}{2}\right)\sin\frac{5\theta}{2}+\frac{5D}{2}\sin\left(\frac{\theta}{2}\right)\right],\quad \Psi_7(r,\theta)=r^{7/2}\left[\left(1-\frac{5D}{2}\right)\sin\frac{7\theta}{2}+\frac{7D}{2}\sin\left(\frac{3\theta}{2}\right)\right].$$

A similar combined method with $L=1$ was used in Karageorghis et al. [3,30].

Since the FS do not satisfy the boundary conditions on $\overline{OD}\cup\overline{OA}$, the algorithms of the MFS and the combined Trefftz method are modified as follows. Define the boundary energy

$$\hat{I}_1(u,v)=\hat{I}(u,v)+\hat{\int}_{\overline{OA}}[v^2+w^2u_y^2]+\hat{\int}_{\overline{OD}}[w^2(\sigma_{xy}^2+\sigma_y^2)], \tag{7.3}$$

where $\hat{I}(u,v)$ is given in (5.4). Denote V_{N-L} the sets of the functions in (7.1) and (7.2). The combined Trefftz method reads: To seek $(u_{N-L},v_{N-L})\in V_{N-L}$ such that

$$\hat{I}_1(u_L,v_L)=\min_{(u,v)\in V_{N-L}}\hat{I}_1(u,v), \tag{7.4}$$

called the combined Trefftz method with FS and singular PS.

We may also establish the collocation equations of u_{N-L} and v_{N-L}, to satisfy (4.13)–(4.16) directly. The collocation equations on $\overline{AB}\cup\overline{BC}\cup\overline{CD}$ are similar to those in Section 5. Here we only give the collocation equations on $\overline{OA}\cup\overline{OD}$. Let $\overline{OA}$ be divided uniformly into small sections with the length h. Denote $h=1/N$. On $\overline{OA}$, let $Q_i = (x_i, 0)$ denote the middle nodes of the small sections, we may have the following collocation equations from (4.14):

$$\sqrt{h}\{v_{N-L}(x_i,0)\}=0,\quad (x_i,0)\in\overline{OA}, \tag{7.5}$$

$$w\sqrt{h}\frac{\partial}{\partial y}\{u_{N-L}(x_i,0)\}=0,\quad (x_i,0)\in\overline{OA}. \tag{7.6}$$

Similarly, for the boundary condition (4.13), let $Q_i=(x_i,0)\in\overline{OD}$ denote the middle nodes of the small sections, we have

$$w\sqrt{h}\{\sigma_{xy}(x_i,0)\}=0,\quad (x_i,0)\in\overline{OD}, \tag{7.7}$$

$$w\sqrt{h}\{\sigma_y(x_i,0)\}=0,\quad (x_i,0)\in\overline{OD}. \tag{7.8}$$

In computation, we will use the method of particular solutions (MPS) in Section 5, the method of fundamental solutions (MFS) and the combined Trefftz method for Models C and D. When $L=0$ in (7.1) and (7.2), Eq. (7.4) leads to the MFS. For the case when $N>0$ and $L>0$, Eq. (7.4) leads to the combined Trefftz method with FS and singular PS with $L\le 4$. In this section, we may choose all FS and only the principal FS by two cases in (7.1) and (7.2): Case (1) four coefficients: a_j, b_j,c_j and d_j, called the combined Trefftz method with c_j, and Case (2) three coefficients: a_j, b_j and d_j, called the combined Trefftz method without c_j.

7.2. Numerical results for Model C

We choose $\lambda=\mu=1$ and the constant $D=\frac{1}{2}$ for the plane strain problems. First we use the MPS in Section 5. Errors, condition numbers and the leading singular coefficient b_1 are listed in Table 1, where $\delta(u)=u_L-u$ and $\delta(v)=v_L-v$, where (u,v) and (u_L, v_L) are the exact and the numerical solutions, respectively. In Table 1, M denotes the number of uniform collocation nodes along the edge $\overline{AB}$ of ∂S in Fig. 1. Then the total number of collocation equations is $m =$ [illegible] On the other hand, for the combined Trefftz method, the number of unknown coefficients in (7.1) and (7.2) is $n = 3N+L+1$ in Case (1) or $n = 2N+L+1$ in Case (2)). In computation, we always choose $m>n$, to obtain the overdetermined system (5.12). By trial computation, a good matching between L and M is found as L:M=4:3 for the MPS. All

Table 1
Errors, condition numbers and the leading coefficient b_1 for Model C by the MPS.

L	M	$\|\varepsilon\|_B$	$\|\delta(u)\|_{\infty,\overline{AB}\cup\overline{CD}}$	$\|\delta(v)\|_{\infty,\overline{BC}}$	Cond	Cond_eff	b_1
4	3	3.85(−2)	3.42(−2)	2.94(−2)	1.88(1)	1.48	**1.14**368836255721
12	9	1.60(−4)	1.65(−4)	1.44(−4)	1.24(3)	3.69	**1.1485**9098444923
20	15	1.55(−6)	1.75(−6)	1.42(−6)	4.61(4)	6.63	**1.1485847**5925981
28	21	1.71(−8)	2.17(−8)	1.80(−8)	1.30(6)	9.83	**1.148584730**04890
36	27	1.93(−10)	2.74(−10)	2.33(−10)	3.14(7)	1.31(1)	**1.14858473018**309
44	33	2.20(−12)	3.51(−12)	2.99(−12)	6.97(8)	1.64(1)	**1.148584730188**89

In the tables, the digits in [illegible] are the significant digits.

Table 2
The leading coefficients for Model C by the MPS as $L=44$, where "Sig" denotes the number of significant digits.

i	All digits	Sig	i	All digits	Sig
0	**−2.370428262538**87(−1)	13	45	**1.99**687020337076(−9)	3
1	**1.1485847301888**9	14	46	**1.5025**6858068054(−8)	5
2	**−2.88315846587**120(−1)	12	47	**−1.581**79639470985(−8)	4
3	**5.19230841152**232(−1)	12	48	**8.28**057992838551(−9)	3
4	**−1.53415881597**239(−1)	12	49	**−4.7**6667024972482(−10)	2
5	**6.770037452**13940(−2)	10	50	**−3.62**297711631423(−9)	3
6	**1.1479885099**1401(−2)	11	51	**4.10**287873062860(−9)	3
7	**−4.3785048274**8510(−2)	11	52	**−1.98**142630852048(−9)	3
8	**3.37958229691**602(−2)	12	53	**9**.74907882476022(−11)	1
9	**−1.4100568779**4208(−2)	11	54	**8.75**529253145755(−10)	3
10	**−5.8848190340**9345(−3)	11	55	**−9**.13866915696900(−10)	1
11	**1.1775997767**1647(−2)	11	56	**4**.74642170185004(−10)	1
12	**−4.4799089939**8035(−3)	11	57	**−2**.27640142183250(−11)	1
13	**3.74054728**462458(−4)	9	58	**−2.11**775542620697(−10)	3
14	**1.5931288123**7556(−3)	11	59	**2.3**5035690132099(−10)	2
15	**−1.662338364**19907(−3)	10	60	**−1.1**3582950021688(−10)	2
16	**9.097707272**99532(−4)	10	61	**4.5**8226081323832(−12)	2
17	**−1.31719582**874128(−4)	9	62	**5**.10703498971552(−11)	1
18	**−3.383193095**17876(−4)	10	63	**−5**.25859160239121(−11)	1
19	**4.8065633**6555710(−4)	8	64	**2**.68661648247200(−11)	1
20	**−2.27593540**644773(−4)	9	65	−8.48080765247575(−13)	0
21	**3.4264744**7930982(−5)	8	66	**−1**.22470315008639(−11)	1
22	**7.72490986**509751(−5)	9	67	**1**.31389685752388(−11)	1
23	**−9.1451781**0538504(−5)	8	68	−6.21584428094673(−12)	0
24	**5.16036598**785792(−5)	9	69	1.43976906315165(−13)	0
25	**−6.917549**27399720(−6)	7	70	**2**.81787036243148(−12)	1
26	**−1.9040845**2201943(−5)	8	71	−2.79023769558602(−12)	0
27	**2.45084454**255830(−5)	9	72	1.35947079331015(−12)	0
28	**−1.1448187**2834006(−5)	8	73	1.33874253203667(−14)	0
29	**9.43584**642064418(−7)	6	74	−6.40094274224709(−13)	0
30	**4.595846**92378893(−6)	7	75	6.29271615723842(−13)	0
31	**−4.95296**448464954(−6)	6	76	−2.70687771833839(−13)	0
32	**2.644074**92708462(−6)	7	77	−6.21110160030781(−15)	0
33	**−2.250543**55949790(−7)	7	78	1.18757456384154(−13)	0
34	**−1.088000**14868308(−6)	7	79	−1.04141378264969(−13)	0
35	**1.306930**10691647(−6)	7	80	4.54353743909940(−14)	0
36	**−6.2282**9320333868(−7)	5	81	3.76241197374834(−15)	0
37	**4.4733**6433498063(−8)	5	82	−2.16115954229057(−14)	0
38	**2.594116**49705148(−7)	7	83	1.78535440243276(−14)	0
39	**−2.7730**5022569719(−7)	5	84	−5.80692324867016(−15)	0
40	**1.4685**0837860825(−7)	5	85	−8.91636465692689(−16)	0
41	**−1.0402**0077396543(−8)	5	86	2.02952876832781(−15)	0
42	**−6.2376**8327081643(−8)	5	87	−9.46300108020484(−16)	0
43	**7.242**21866528618(−8)	4	88	2.42754765979950(−16)	0
44	**−3.475**68682058097(−8)	4			

computations in this paper are calculated by double precision. Table 2 lists the leading coefficients b_i by the MPS in Section 5, where the digits in bold denote significant digits, compared with the higher accuracy of b_i obtained by using $L=200$ with 500 working digits. The singular leading coefficient b_1 has 14 significant digits:

$$b_1 = \mathbf{1.1485847301888}9. \tag{7.9}$$

From Table 1 we can see the asymptotes

$$\|\varepsilon\|_B = O((0.57)^L), \quad \|\delta(u)\|_{\infty,\overline{AB}\cup\overline{CD}} = O((0.58)^L), \quad \|\delta(v)\|_{\infty,\overline{BC}} = O((0.58)^L), \tag{7.10}$$

$$\text{Cond} = O((1.48)^L), \quad \text{Cond\_eff} = O((1.03)^L). \tag{7.11}$$

In (7.10) and (7.11), the boundary errors of the MPS is defined as

$$\|\varepsilon\|_B^2 = \int_{\overline{BC}} [(\tilde{v}-1)^2 + w^2 \tilde{u}_y^2] + \int_{\overline{AB}\cup\overline{CD}} [\tilde{u}^2 + w^2 \tilde{v}_x^2], \tag{7.12}$$

where $\tilde{u}$ and $\tilde{v}$ are the numerical solutions.

Below, we use the FS. Based on the analysis in Bogomolny [4] and Li [40], the source points of FS may be located uniformly on a circle ℓ_R outside of the solution domain S. Choose $(0, \frac{1}{2})$ as the origin of ℓ_R and the radius $R > \sqrt{1+\frac{1}{4}} = 1.118$ (see Fig. 1). By trial computation, we have found a good radius $R=1.4$ to balance accuracy and stability. Also by trial computation, some good matches between N and M with $L \le 4$ have been found, which are used in Tables 3–5. Details of numerical results are omitted. First we apply the MFS (i.e., $L=0$ in (7.1) and (7.2)), and list the results in Table 3. The errors are large, compared with Table 1, since the solution near the crack point is singular,

Table 3
Errors and condition numbers for Model C by the MFS with c_j and $R=1.4$.

N	M	$\|\varepsilon\|_B$	$\|\delta(u)\|_{\infty,\overline{AB}\cup\overline{CD}}$	$\|\delta(v)\|_{\infty,\overline{BC}}$	Cond	Cond_eff
4	3	4.68(−1)	1.85(−1)	3.21(−1)	1.86(1)	6.56
12	9	1.20(−1)	2.88(−2)	1.82(−1)	9.18(2)	3.88(1)
20	15	6.91(−2)	9.01(−3)	1.36(−1)	3.71(4)	1.69(2)
28	21	4.81(−2)	4.13(−3)	1.11(−1)	2.23(6)	6.25(2)
36	27	3.70(−2)	4.11(−3)	9.47(−2)	2.37(8)	3.31(3)
44	33	2.98(−2)	4.65(−3)	8.31(−2)	1.52(10)	6.29(3)

Table 4
Errors and condition numbers for Model C by the combined Trefftz method with c_j at $R=1.4$ and $L\le 4$.

N	M	L	$\|\varepsilon\|_B$	$\|\delta(u)\|_{\infty,\overline{AB}\cup\overline{CD}}$	$\|\delta(v)\|_{\infty,\overline{BC}}$	Cond	Cond_eff	d_1
4	3	2	1.91(−1)	1.64(−1)	1.22(−1)	2.45(1)	5.67	0.90492074481298
12	9	2	7.35(−3)	3.57(−3)	4.19(−3)	1.46(3)	1.62(2)	**1.1**5343841994475
20	15	3	5.14(−4)	5.26(−4)	8.70(−4)	3.81(4)	3.43(3)	**1.14**742779006686
28	21	3	4.15(−5)	7.36(−5)	4.24(−5)	2.27(6)	4.81(4)	**1.148**19838807392
36	27	4	2.38(−6)	4.25(−6)	2.58(−6)	2.39(8)	1.20(6)	**1.1485**7021388897
44	33	4	4.23(−7)	5.93(−7)	5.61(−7)	1.52(10)	1.07(7)	**1.14858**201640097

Table 5
Errors and condition numbers for Model C by the combined Trefftz method without c_j at $R=1.4$ and $L\le 4$.

N	M	L	$\|\varepsilon\|_B$	$\|\delta(u)\|_{\infty,\overline{AB}\cup\overline{CD}}$	$\|\delta(v)\|_{\infty,\overline{BC}}$	Cond	Cond_eff	d_1
6	3	2	8.67(−2)	7.14(−2)	7.23(−2)	3.39(1)	7.87	**1.1**5112753961336
18	9	2	3.93(−3)	3.18(−3)	3.40(−3)	1.19(3)	1.63(2)	**1.1**3569064110089
30	15	3	1.70(−4)	2.03(−4)	1.88(−4)	1.18(5)	1.13(4)	**1.148**00722494228
42	21	3	7.93(−6)	1.75(−5)	8.59(−6)	1.05(7)	6.14(5)	**1.1485**3380776012
54	27	4	4.97(−7)	1.69(−6)	5.77(−7)	8.33(8)	1.23(7)	**1.14858**269715584
66	33	4	2.52(−8)	9.89(−8)	7.29(−8)	6.69(10)	1.79(8)	**1.148584**95869961

but the fundamental solutions are smooth. Next, we use the combined Trefftz method with many FS and a few singular PS. Tables 4 and 5 list the results of the combined method of two cases with and without c_j in (7.1) and (7.2).

We cite the last row in Table 5 with $N=66$ and $L\le 4$,

$$\|\varepsilon\|_B=2.52(-8),\quad \|\delta(u)\|_{\infty,\overline{AB}\cup\overline{CD}}=9.89(-8),\quad \|\delta(v)\|_{\infty,\overline{BC}}=7.29(-8), \tag{7.13}$$

$$\mathrm{Cond}=6.69(10),\quad \mathrm{Cond_eff}=1.79(8),$$

$$d_1=\mathbf{1.148584}95869961. \tag{7.14}$$

Compared with the high accurate coefficient (7.9), the leading singular coefficient d_1 in (7.14) has seven significant digits. The errors $O(10^{-7})$ of displacements are small, and the effective condition numbers as $O(10^8)$ are moderate for $N=66$ and $L=4$. By double precision and four singular particular solutions used, such numerical solutions are, indeed, excellent, to show the significance of the algorithms proposed in this paper. More importantly, for other corners $\Theta\ne\pi$ in linear elastostatics, a few singular solutions can be easily found, see [43]. Then the combined Trefftz method also has a wide scale of applications.

In (7.13), $\delta(u)=u-u_{N-L}$, $\delta(v)=v-v_{N-L}$, where u and v are the exact solutions which can be obtained from Table 2, and u_{N-L} and v_{N-L} are the numerical solutions by the combined Trefftz method. The boundary errors are defined as

$$\|\varepsilon\|_B^2=\int_{\overline{BC}}[(\tilde v-1)^2+w^2\tilde u_y^2]+\int_{\overline{AB}\cup\overline{CD}}[\tilde u^2+w^2\tilde v_x^2]+\int_{\overline{OA}}[\tilde v^2+w^2\tilde u_y^2]+\int_{\overline{OD}}[w^2(\tilde\sigma_{xy}^2+\tilde\sigma_y^2)], \tag{7.15}$$

where $\tilde u,\tilde v,\tilde\sigma_{xy}$ and $\tilde\sigma_y$ are the numerical solutions of displacement and stress. From Tables 4 and 5, there seems to exist no significant differences of errors and condition numbers between the solutions from the combined Trefftz method in two cases. Strictly speaking, however, Table 5 without c_j in cases (2), the accuracy of d_1 and the solutions are slightly higher, but the instability is slightly worse. An important consequence is that we may choose only the principal FS in computation, as done in [3,30,31].

Note that the true errors in Tables 3–6 can be evaluated, based on the highly accurate solutions in Table 2 by the CTM for Model C. This displays a significance of the singularity models in evaluations and developments of new and efficient numerical solutions (also see [38]). Besides, for the MPS, the effective condition number Cond_eff is significantly smaller than the traditional condition number Cond (see Table 3). Unfortunately, such a situation does not remain for the MFS and the combined Trefftz method (see Tables 4 and 5). Since the Cond_eff is a better criterion for numerical stability [42], we conclude that the stability of the MPS is much better than that of the combined Trefftz method. Under double precision, the results in Tables 4 and 5 with four singular PS are excellent; this also proves the importance of FS for singularity problems of linear elastostatics.

Please cite this article as: Lee M-G, et al. Combined Trefftz methods of particular and fundamental solutions for corner and crack singularity of linear elastostatics. Eng Anal Bound Elem (2010), doi:10.1016/j.enganabound.2010.02.005

7.3. Numerical results for Model D

For Model D, the singular solutions (4.17) and (4.18) are chosen to replace (4.11) and (4.12). Methods of MPS and the combined Trefftz method with may FS and a few singular PS are used. Numerical results are listed in Tables 6–9. Under double precision, by the MPS and the combined Trefftz combined method, the singular leading coefficients a_1 has 12 and 6 significant digits, respectively. The analysis and conclusions are similar to those for Model C in Section 7.2.

Table 6
Errors, condition numbers and the leading coefficient a_1 for Model D by the MPS.

L	M	$\Vert\varepsilon\Vert_B$	$\Vert\delta(u)\Vert_{\infty,\overline{AB}\cup\overline{CD}}$	$\Vert\delta(v)\Vert_{\infty,\overline{BC}}$	Cond	Cond_eff	a_1
4	3	1.25(−2)	7.81(−3)	9.55(−3)	1.03(2)	1.54(1)	−**6.**29744043262435(−1)
12	9	6.16(−5)	3.28(−5)	8.41(−5)	9.92(3)	5.48(1)	−**6.425**70862370564(−1)
20	15	5.54(−7)	4.74(−7)	8.68(−7)	3.46(5)	9.14(1)	−**6.42516**309256916(−1)
28	21	5.57(−9)	3.98(−9)	1.09(−8)	9.23(6)	1.28(2)	−**6.4251610**3733957(−1)
36	27	5.85(−11)	3.46(−11)	1.40(−10)	2.16(8)	1.65(2)	−**6.42516105**797704(−1)
44	33	6.25(−13)	4.26(−13)	1.76(−12)	4.70(9)	2.01(2)	−**6.42516105845**949(−1)

Table 7
The leading coefficients for Model D by the MPS as L=44, where “Sig” denotes the number of significant digits.

i	All digits	Sig	i	All digits	Sig
0	**3.00824180850**544(−1)	12	45	**3.2**9496672296780(−10)	2
1	**−6.42516105845**949(−1)	12	46	**8.82**155089981674(−9)	3
2	**1.1455860355663**4(−1)	14	47	**−8.88**165040485921(−9)	3
3	**−9.055961315**45387(−2)	10	48	**4.46**915200554410(−9)	3
4	**−1.00133266806**236(−1)	12	49	**−6**.56063755125505(−11)	1
5	**4.312877274**66098(−2)	10	50	**−2.11762**964068200(−9)	6
6	**8.8376805484**6057(−3)	11	51	**1.96**081428354774(−9)	3
7	**−2.9252168234**9179(−2)	11	52	**−1.07**119483830204(−9)	3
8	**2.1751501117**0407(−2)	11	53	**1**.54875940543816(−11)	1
9	**−2.659760985**69854(−3)	10	54	**5.100**16926677634(−10)	4
10	**−4.496875699**25360(−3)	10	55	**−5.1**2068209255339(−10)	2
11	**3.486112528**71003(−3)	10	56	**2.5**6396300001414(−10)	2
12	**−2.667577150**11588(−3)	10	57	−2.22058041989034(−12)	0
13	**−6.9776224**6370839(−5)	8	58	**−1.230**99907653652(−10)	4
14	**1.186441638**73355(−3)	10	59	**1**.14213243884390(−10)	1
15	**−1.0499460219**3778(−3)	11	60	**−6**.07763289167005(−11)	1
16	**4.86211482**873922(−4)	9	61	−5.08543467519319(−14)	0
17	**1.072560**87919489(−5)	8	62	**2.98**045250136169(−11)	3
18	**−2.36520994**891771(−4)	9	63	**−2**.92515464971986(−11)	1
19	**1.80922805**236206(−4)	9	64	1.41409263344311(−11)	0
20	**−1.18594689**892560(−4)	9	65	3.62833209866620(−13)	0
21	**7.1582297**8719642(−6)	8	66	**−7**.13473692009601(−12)	1
22	**5.00212342**652693(−5)	9	67	6.26515741724242(−12)	0
23	**−5.218042648**51576(−5)	10	68	−2.99503004677283(−12)	0
24	**2.6982494**9614390(−5)	8	69	−2.97916861068619(−13)	0
25	**−9.32611**720837695(−7)	6	70	**1**.73631665525185(−12)	1
26	**−1.1807636**0100786(−5)	8	71	−1.52409417845515(−12)	0
27	**1.018396020**85493(−5)	10	72	6.29773910581016(−13)	0
28	**−6.037022**07083258(−6)	7	73	1.08296316663771(−13)	0
29	**1.17179**588105640(−7)	6	74	**−3**.77558122856455(−13)	1
30	**2.795418**98566603(−6)	7	75	2.58615118820145(−13)	0
31	**−2.79857**743366890(−6)	6	76	−6.56170861407564(−14)	0
32	**1.404791**85322274(−6)	7	77	−6.52198268913219(−14)	0
33	**−2.4191**7675474903(−8)	5	78	9.35980663684149(−14)	0
34	**−6.53545**380884399(−7)	6	79	−5.88528705672714(−14)	0
35	**5.81627**035831825(−7)	6	80	1.45281463147242(−14)	0
36	**−3.3267**2038714524(−7)	5	81	9.67563429120815(−15)	0
37	**7.827**51738954602(−9)	4	82	−1.28690752944223(−14)	0
38	**1.542990**45199128(−7)	7	83	3.94406449501058(−15)	0
39	**−1.5599**2977258194(−7)	5	84	3.63401780375346(−15)	0
40	**7.876**20815941885(−8)	4	85	−5.23106667805297(−15)	0
41	**−1.44**590834394496(−9)	3	86	3.38106737743343(−15)	0
42	**−3.6828**2126035862(−8)	5	87	−1.17175934824599(−15)	0
43	**3.362**24233066243(−8)	4	88	1.31129249701619(−16)	0
44	**−1.870**69208889886(−8)	4			

Table 8
Errors and condition numbers for Model D by the combined Trefftz method with c_j at $R=1.4$ and $L \le 4$.

N	M	L	$\|\varepsilon\|_B$	$\|\delta(u)\|_{\infty,\overline{AB}\cup\overline{CD}}$	$\|\delta(v)\|_{\infty,\overline{BC}}$	Cond	Cond_eff	d_1
4	3	2	4.12(−2)	1.40(−2)	2.40(−2)	3.63(1)	1.40(1)	−**6.**76367717749435(−1)
12	9	2	5.27(−3)	2.81(−3)	5.56(−3)	2.99(3)	4.42(2)	−**6.**29466787915089(−1)
20	15	3	3.18(−4)	5.94(−4)	2.81(−4)	4.86(4)	5.95(3)	−**6.42**638017460067(−1)
28	21	3	1.80(−5)	3.61(−5)	2.11(−5)	3.33(6)	1.14(5)	−**6.42**629905018329(−1)
36	27	4	8.34(−7)	9.68(−7)	1.99(−6)	3.06(8)	6.43(6)	−**6.425**32091601947(−1)
44	33	4	1.24(−7)	1.33(−7)	1.77(−7)	2.18(10)	4.26(7)	−**6.42517**844619497(−1)

Table 9
Errors and condition numbers for Model D by the combined Trefftz method without c_j at $R=1.4$ and $L \le 4$.

N	M	L	$\|\varepsilon\|_B$	$\|\delta(u)\|_{\infty,\overline{AB}\cup\overline{CD}}$	$\|\delta(v)\|_{\infty,\overline{BC}}$	Cond	Cond_eff	d_1
6	3	2	3.47(−2)	2.95(−2)	1.35(−2)	5.51(1)	2.10(1)	−**6.**59581243246061(−1)
18	9	2	2.80(−3)	2.57(−3)	3.47(−3)	1.83(3)	4.16(2)	−**6.**29196116420615(−1)
30	15	3	7.26(−5)	8.79(−5)	5.21(−5)	2.00(5)	3.41(4)	−**6.42**461567607067(−1)
42	21	3	3.53(−6)	5.67(−6)	6.64(−6)	1.73(7)	1.24(6)	−**6.425**42596419065(−1)
54	27	4	2.16(−7)	5.30(−7)	7.33(−7)	1.52(9)	3.19(7)	−**6.425**21862472346(−1)
66	33	4	1.25(−8)	3.07(−8)	4.96(−8)	1.26(11)	5.68(8)	−**6.42516**049509492(−1)

7.4. A brief error analysis

In this subsection section, a brief error analysis is given for the combined Trefftz methods with many FS and a few singular PS; strict analysis will be given elsewhere.

Let the small L be fixed. Since the leading singularity of the solutions can be matched perfectly in the combined Trefftz methods, the rest solutions u^{Δ} have the singularity $O(r^{L+1/2})$, which implies $u^{\Delta} \in H^{L+1-\delta}(\partial S)$ and $u^{\Delta} \in H^{L+3/2-\delta}(S)$, where $0<\delta \ll 1$, and $H^k(\partial S)$ and $H^k(S)$ are the Sobolev norms. Since the smooth fundamental solutions play a role in approximation as the polynomials do by following Li [38,40], when $w=1/N$ we can derive the errors

$$\|\varepsilon\|_B = O\left(\frac{1}{N^{L+1-\delta}}\right), \tag{7.16}$$

$$\|\varepsilon\|_1 = \{\|u-u_N\|^2_{1,S} + \|v-v_N\|^2_{1,S}\}^{1/2} = O\left(\frac{1}{N^{L+1/2-\delta}}\right), \tag{7.17}$$

where $\|u\|_{1,S}$ is the Sobolev norm in H^1 space. When $L=0$, we have from (7.16) and (7.17)

$$\|\varepsilon\|_B = O\left(\frac{1}{N^{1-\delta}}\right), \quad \|\varepsilon\|_1 = O\left(\frac{1}{N^{1/2-\delta}}\right). \tag{7.18}$$

The errors of $\|\varepsilon\|_B$ in Table 3 decrease slowly, just as $O(1/N)$. When $L=1$ as in [30], the better errors are given by

$$\|\varepsilon\|_B = O\left(\frac{1}{N^{2-\delta}}\right), \quad \|\varepsilon\|_1 = O\left(\frac{1}{N^{3/2-\delta}}\right). \tag{7.19}$$

When $L=4$, we have the small errors from (7.16) and (7.17),

$$\|\varepsilon\|_B = O\left(\frac{1}{N^{5-\delta}}\right), \quad \|\varepsilon\|_1 = O\left(\frac{1}{N^{4.5-\delta}}\right). \tag{7.20}$$

Suppose that for $L=4$, the errors of the solutions from the combined Trefftz method satisfy

$$\|\varepsilon\|_B \le C_1 \frac{1}{N^5}, \tag{7.21}$$

where C_1 is a constant independent of N. We can see the last two rows in Table 5 for $N=54$, 66,

$$\|\varepsilon\|_B = O(10^{-7}), \quad O(10^{-8}). \tag{7.22}$$

On the other hand, for $N=54$, 66 we have

$$\frac{1}{N^5} = O(10^{-9}), \quad O(10^{-10}). \tag{7.23}$$

Comparing (7.23) with (7.22), from (7.21) we conclude the constant $C_1 = O(10^2)$.

Next, let us consider the errors Δb_1 of the leading singular coefficient b_1. From Li [38], we have

$$|\Delta b_1| = O(\|\varepsilon\|_1) = O\left(\frac{1}{N^{L+1/2-\delta}}\right). \tag{7.24}$$

For $L=4$, we assume

$$|\Delta b_1| \le C_2 \frac{1}{N^{4.5}}, \tag{7.25}$$

with a constant C independent of N. Compared the data of b_1 with the accurate value in (7.9), we can see for $N=54$, 66 from Table 5,

$$|\Delta b_1| = O(10^{-6}), \quad O(10^{-7}). \tag{7.26}$$

Since for $N=54$, 66,

$$\frac{1}{N^{4.5}} = O(10^{-8}), \quad O(10^{-9}). \tag{7.27}$$

we also conclude the constant $C_2 = O(10^2)$.

When small L varies and grows very slowly as in Tables 4 and 5, under a certain coupling between N and L, we may also derive the errors bounds; details are omitted. The above analysis supports the excellence of numerical results obtained by the combined Trefftz method.

Remark 7.1. In this section, we have explored how to effectively apply the FS to the singularity problems of linear elastostatics. Based on the numerical results and a brief error analysis, the combined Trefftz methods with many FS and a few singular PS are strongly recommended, where both FS and PS are used in the entire solution domain. This is distinct from the combinations of MFS and MPS, where FS and PS are used in two subdomains, separately, and the coupling techniques are adopted along their common boundary (see [38,39]). It is worth pointing out that the numerical results by the combined Trefftz method in this paper are excellent, and its algorithms can be easily extended to general corner problems of linear elastostatics. Moreover, from Theorem 2.1, the complete set of FS is given in (6.9) and (6.10). Interestingly, from Tables 4 and 5, we may conclude that to ignore $[(x-\xi_i)/r_i^2,(y-\eta_i)/r_i^2]^T$ (i.e., $c_j = 0$) and to choose only the principal FS in Cases (2) do not provide a worse impact on the numerical solutions, thus to support some numerical algorithms and results in [30,31].

8. Concluding remarks

To close this paper, let us made a few concluding remarks.

1. In this paper and [43], we provide a systematic analysis, not only for singularity properties and particular solutions of linear elastostatics at corners, but also for the MFS for both smooth and singularity problems. In this paper, the corners with free traction boundary conditions are discussed, to derive more general particular solutions than those in [43].
2. In Section 3, the complex representation of particular solutions and stress are explored, and the *general* particular solutions at the corners with free traction boundary conditions are derived, directly from the Cauchy–Navier equation of linear elastostatics. The new Model D is obtained only from this paper. Note that the singularity analysis in this paper is distinct to that in Williams [67,48] by using a similarity to biharmonic equations, although the results are coincident with each other. The explicit particular solutions at the crack tip under free taction conditions in this paper are also equivalent to the explicit complex solutions in Pitner [55].
3. Two new models are designed, called Models C and D. Their highly accurate solutions are obtained by the collocation Trefftz methods (CTM), and the leading singular coefficients reach 12–14 significant digits by the computation in double precision, see Tables 2 and 7. Those accurate solutions can be used, to examine other numerical solutions for singularity problems as in [38] and in Section 7 for the combined Trefftz method.
4. The fundamental solutions (FS) of linear elastostatics are explored in Section 6, where the FS are derived in detail, the equivalence of FS to the complex representation in [52,31] is proved, and the proof of FS satisfying the Cauchy–Navier equations in 2D is provided. The analysis in Sections 6 and 7 can be regarded as a theoretical foundation of FS for smooth and singular solutions of linear elastostatics.
5. In Section 7, for the crack singularity, the combined Trefftz method with many FS and a few singular PS (say, four terms) are proposed, to give the leading singular coefficient with seven (or six) significant digits, and the solution errors with $O(10^{-7})$ under double precision. Since for the corners with $\Theta \neq \pi$, the powers v_k in r^{v_k} have to be computed in advance, to find many particular solutions is difficult and troublesome. Therefore, the combined Trefftz method proposed in this paper may be applied to all corner singularity of linear elastostatics. Evidently, the analysis and computation in this paper not only display significance of the singular solutions, but also extend widely the applications of the MFS.
6. This paper also displays the importance of the FS for linear elastostatics. For smooth problems, the method of particular solutions (MPS) is superior to the method of fundamental solutions (MFS), because the ill-conditioning of the MFS is severe [47]. For singularity problems of linear elastostatics, however, the FS is also important, because using the FS is *advantageous* for the corners with $\Theta \neq \pi$. Since the leading singular particular solutions are used in the Trefftz combined methods, to match well the principal singularity of the solutions, we do not needed so many FS, thus to relieve the ill-conditioning, see Tables 4 and 5. Sections 6 and 7 have provided a systematic analysis of the FS for theory and computation of linear elastostatics.
7. The analysis, numerical algorithms and numerical results of this paper with [43] may greatly enrich both linear elastostatics theory with corner and numerical methods, such as the combined method [30,38,39] and the Trefftz methods [65,1,5,10,8,11,15,16,49,50,58,62,68], which also include the boundary approximation method [37,45], the collocation Trefftz method [43], the method of fundamental solutions [6,5,10,9,17–20,33,30,31,34,35,63,64,61], the hybrid Trefftz method [22,23,27–29,60], the boundary collocation techniques [32], the Trefftz-BEM [13,66], the dual method [57], etc.

References

[1] Akella MR, Kotamraju GR. Trefftz indirect method applied to nonlinear potential problems. Eng Anal Bound Elem 2000b;24:459–65.
[2] Alduncin G, Herrera I. Contribution to free boundary problems using boundary elements: Trefftz approach. Comput Methods Appl Mech Eng 1984b;42:257–71.

Please cite this article as: Lee M-G, et al. Combined Trefftz methods of particular and fundamental solutions for corner and crack singularity of linear elastostatics. Eng Anal Bound Elem (2010), doi:10.1016/j.enganabound.2010.02.005

Q3 [3] Berger JR, Karageorghis A, Martin PA. Stress intensity factor computation using the method of fundamental solution: mixed-mode problem 2007b;69:469–83.
[4] Bogomolny A. Fundamental solutions method for elliptic boundary value problems. SIAM J Numer Anal 1985b;22:644–69.
[5] Chen CS, Hon YC, Schaback RA. Scientific computing with radial basis functions. Preprint, Department of Mathematics, University of Southern Mississippi, Hattiesburg, MS, USA, 2005.
[6] Chen CS, Karageorghis A, Smyrlis YS, editors. The method of fundamental solutions—a meshless method. USA: Dynamic Publishers, Inc.; 2009.
[7] Chen G, Zhou J. Boundary element methods. New York: Academic Press; 1992. [Chapter 9].
[8] Chen JT, Lee YT, Shieh SC. Revisit of two classical elasticity problems by using the Trefftz method. Eng Anal Bound Elem 2009b;33:890–5.
[9] Chen JT, Lee YT, Yu SR, Shieh SC. Equivalence between the Trefftz method and the method of fundamental solution for the annular Green's function using the addition theorem and image concept. Eng Anal Bound Elem 2009b;33:678–88.
[10] Chen JT, Wu CS, Lee YT, Chen KH. On the equivalence of the Trefftz method and method of fundamental solutions for Laplace and biharmonic equations. Comput Math Appl 2007b;53:851–79.
[11] Chen YW, Liu CS, Chang JR. Applications of the modified Trefftz method for the Laplace equation. Eng Anal Bound Elem 2009b;33:137–46.
[12] Choi N, Choo YS, Lee BC. A hybrid Trefftz plane elasticity element with drilling degrees of freedom. Comput Methods Appl Mech Eng 2006b;195:4095–105.
[13] Cui YH, Wang J, Dhanasekar M, Qin QH. Model III fracture analysis by Trefftz boundary element method. Acta Mech Sin 2007b;23:173–81.
[14] Domingues JS, Portela A, de Castro PMST. Trefftz boundary element method applied to fracture mechanics. Eng Fract Mech 1999b;64:67–86.
[15] Dong CY, Lo SH, Cheung YK, Lee KY. An isotropic thin plate bending problems by Trefftz boundary collocation method. Eng Anal Bound Elem 2004b;28:1017–24.
[16] Elliotis M, Georgiou G, Xenophontos C. The singular function boundary integral method for biharmonic problems with crack singularities. Eng Anal Bound Elem 2007b;31:209–15.
[17] Fairweather G, Karageorghis A. The method of fundamental solutions for numerical solutions of the biharmonic equation. J Comput Phys 1987b;69:434–59.
[18] Fairweather G, Karageorghis A. The Almani method of fundamental solutions for solving biharmonic problems. Int J Numer Methods Eng 1988b;26:1665–82.
[19] Fairweather G, Karageorghis A. The simple layer potential method of fundamental solutions for certain biharmonic problems. Int J Numer Methods Eng 1989b;9:1221–34.
[20] Fairweather G, Karageorghis A. The method of fundamental solutions for elliptic boundary value problems. Adv Comput Math 1998b;9:69–95.
[21] de Freitas JAT. Formulation of elastostatic hybrid-Trefftz stress elements. Comput Methods Appl Mech Eng 1998b;153:127–51.
[22] de Freitas JAT, Ji ZY. Hybrid-Trefftz finite element formulation for simulation of singular stress fields. Int J Numer Meth Eng 1996b;39:281–308.
[23] de Freitas JAT, Ji ZY. Hybrid-Trefftz equilibrium model for crack problems. Int J Numer Meth Eng 1996b;39:569–84.
[24] de Freitas JAT, Toma M. Hybrid-Trefftz stress and displacement elements for axisymmetric incompressible biphasic media. Comput Methods Appl Mech Eng 2009b;198:2368–90.
[25] Hu HY, Li ZC. Collocation methods for Poisson's equation. Comput Methods Appl Mech Eng 2006b;195:4139–60.
[26] Hu HY, Li ZC, Cheng AH-D. Radial basis collocation methods for elliptic boundary value problems. Int J Comput Math Appl 2005b;50:289–320.
[27] Jirousek J, Venkstesh A. Hybrid Trefftz plane elasticity element with p-method capabilities. Int J Numer Eng 1992b;35:1443–72.
[28] Jirousek J, Wroblewski A. T-element: state of the art and future trends. Arch Comput Methods Eng 1996b;3:323–434.
[29] Jirousek J, Wroblewski A, Qin QH, He XQ. A family of quadrilateral hybrid-Trefftz p-elements for thick plate analysis. Comput Methods Appl Mech Eng 1995b;127:315–44.
[30] Karageorghis A, Poulikkas A, Berger JR. Stress intensity factor computation using the method of fundamental solutions. Comput Mech 2006b;37:445–54.
[31] Karageorghis A, Mogilevskaya SG, Stolarski H. On efficient MFS algorithms using complex representations. In: Chen CS, Karageorghis A, Smyrlis YS, editors. The method of fundamental solutions—a meshless method. Atlanta: Dynamic Publishers, Inc.; 2008. p. 107–25. [Chapter 5].
[32] Kolodziej JA, Zielinski AP. Boundary collocation techniques and their application in engineering. Southampton, Boston: WIT press; 2009.
[33] Kupradze VD. Potential methods in elasticity. In: Sneddon JN, Hill R editors, Progress in solid mechanics, vol. III, Amsterdam; 1963. p. 1–259.
[34] Leitao VMA. Applications of multi-region Trefftz-collocation to fracture mechanics. Eng Anal Bound Elem 1998b;22:251–6.
[35] Leitao VMA. Crack analysis using an enriched MFS domain decomposition technique. Eng Anal Bound Elem 2006b;30:160–6.
[36] Li ZC. A combined method for solving elliptic problems on unbounded domains. Comput Methods Appl Mech Eng 1989b;73:191–208.
[37] Li ZC. Numerical methods for elliptic problems with singularities: boundary methods and nonconforming combinations. Singapore: World Scientific; 1990.
[38] Li ZC. Combined methods for elliptic equations with singularities, interfaces and infinities. Boston: Kluwer Academic Publishers; 1998.
[39] Li ZC. Combinations of method of fundamental solutions for Laplace's equation with singularities. Eng Anal Bound Elem 2008b;32:856–69.
[40] Li ZC. Method of fundamental solutions for annual shaped domains. J Comput Appl Math 2008b;228:355–72.
[41] Li ZC, Bui TD. Penalty-combined methods and their applications in solving elliptic problems with singularities. Comput Methods Appl Mech Eng 1992b;97:291–316.
[42] Li ZC, Chien CS, Huang HT. Effective condition number for Finite difference method. J Comput Appl Math 2007b;198:208–35.
Q4 [43] Li ZC, Chu PC, Young LJ, Lee MG. Models of corner and crack singularity of linear elastostatics and their numerical solutions. Eng Anal Bound Elem 2009, accepted for publication.
[44] Li ZC, Lu TT, Hu HY, Cheng AHD. Trefftz and collocation methods. Southampton, Boston: WIT Press; 2009.
[45] Li ZC, Mathon R, Sermer P. Boundary methods for solving elliptic problems with singularities and interfaces. SIAM J Numer Anal 1987b;24:487–98.
[46] Li ZC, Tsai WC, Lee MG, Young LJ. Boundary Methods for coupling traction conditions in linear elastostatics. Technical Report, Department of Applied Mathematics, National Sun Yat-Sen University, Kaohsiung, Taiwan; 2009.
[47] Li ZC, Young HJ, Huang HT, Liu YP, Cheng AH-D. Comparisons of fundamental solutions and particular solutions for Trefftz methods. Eng Anal Bound Elem 2009, accepted for publication.
[48] Lin KY, Tong P. Singular finite element for the fracture analysis of V-notched plate. Int J Numer Meth Eng 1980b;15:1343–54.
[49] Liu CS. An effectively modified direct Trefftz method for 2D potential problems considering the domain's characteristic length. Eng Anal Bound Elem 2007b;31:983–93.
[50] Liu X, Wu X. Differential quadrature Trefftz method for irregular plate problems. Eng Anal Bound Elem 2009b;33:363–7.
[51] Lu TT, Hu HY, Li ZC. Highly accurate solutions of Motz's and the cracked beam problems. Eng Anal Bound Elem 2004b;28:1387–403.
[52] Mogilevskaya SG, Linkov AM. Complex fundamental solutions and complex variables boundary element method in elasticity. Comput Mech 1998b;22:88–92.
[53] Muskhelishvili NI. Some basic problems of the mathematical theory of elasticity, Noordhoff: Groningen, Holland; 1953.
[54] Petrolito J. Hybrid-Trefftz quadrilateral elements for thick plate analysis. Comput Methods Appl Mech Eng 1990b;78:331–51.
[55] Piltner R. Recent developments in Trefftz method for finite element and boundary applications. Adv Eng Software 1995b;24:107–15.
[56] Poitou A, Bouberbachene M, Hochard C. Resolution of three-dimensional Stokes fluid flows using a Trefftz method. Comput Methods Appl Mech Eng 2000b;190:561–78.
[57] Portela A, Alliabadi MH, Rooke DP. The dual boundary element method: effective implementation for crack problems. Int J Numer Meth Eng 1992b;33:1269–87.
[58] Portela A, Charafi A. Trefftz boundary element method for domains with slits. Eng Anal Bound Elem 1997b;20:299–304.
[59] Qin QH. Hybrid-Trefftz finite element method for Reissner plates on an elastic foundation. Comput Methods Appl Mech Eng 1995b;122:379–92.
[60] Qin QH. The Trefftz finite and boundary element method. Southampton, Boston: WIT Press; 2000.
[61] Schaback R. Adaptive numerical solution of MFS systems. In: Chen CS, Karageorghis A, Smyrlis YS, editors. The method of fundamental solutions—a meshless method. Atlanta: Dynamic Publishers, Inc.; 2008. p. 1–27. [Chapter 1].
[62] Shaw RP, Huang SC, Zhao CX. The embedding integral and the Trefftz method for potential problems with partitioning. Eng Anal Bound Elem 1992b;9:83–90.
[63] Smyrilis YS. The method of fundamental solutions, a weighted least-squares approach. BIT Numer Math 2006b;46:163–94.
[64] Smyrilis YS, Karageorghis A. A linear least-squares MFS for certain elliptic problems. Numer Algorithms 2004b;35:29–44.
[65] Trefftz E. Konvergenz und Ritz'schen Verfahren. In: Proceedings of the 2nd International Congress for Applied Mechanics, Znrch, 1926. p. 131–7.
[66] Wang J, Cui YH, Qin QH, Jia JY. Application of Trefftz BEM to anti-plane piezoelectric problem. Acta Mech Sin 2006b;19:352–64.
[67] Williams ML. Stress singularities resulting from various boundary conditions in angular corners of plates in extension. J Appl Mech 1952b;19:526–8.
[68] Wu X, Du H, Kong W. Differential quadrature Trefftz method for Poisson-type problems on irregular domains. Eng Anal Bound Elem 2008b;32:413–23.
[69] Yu DH. Natural boundary integral method and its applications. Beijing/New York: Science Press/Kluwer Academic Publishers; 2002.
[70] Zieliski AP. Trefftz method: elastic and elastoplastic problems. Comput Methods Appl Mech Eng 1988b;69:185–204.